TAMPEREEN TEKNILLINEN YLIOPISTO
TAMPERE UNIVERSITY OF TECHNOLOGY

PERTTI TAPIAINEN

HEAT TRANSFER TESTING OF INSULATED RADIAL SYSTEMS

Master of Science Thesis

Examiners:
Professor Risto Raiko and
Professor Erkki Levänen
Examiners and the subject approved
at the faculty meeting of Natural Sciences on 17.08.2016

ABSTRACT

PERTTI TAPIAINEN:
Heat Transfer Testing of Insulated Radial Systems
Tampere University of Technology
Master of Science Thesis, 50 pages
September 2016
Master's Degree Programme in Environment and Energy Technology
Major: Combustion Technology
Examiners: Professor Risto Raiko and Professor Erkki Levänen

Keywords: thermal conductivity, interface, heat transfer, refractory

The objective of this study was to design and conduct an easily reproducible test method to find out the thermal conductivities of different refractory materials. Another objective was to investigate the interfacial thermal resistances between the steel pipe and the refractory layer to receive better information of the total heat transfer coefficient from the outside surface of the refractory to the insides of the steel pipe.

The test system consisted of an insulated cylindrical oven and a water distribution system with adjustable levels for the temperature, pressure and volume flow of the water circulating inside the test tube. Three different refractory masses were examined as they were casted on top of steel tubes and one of the masses was also used in a test tube with studs installed onto it to examine their effect onto the heat transfer. In addition to the thermal conductivity of the refractory mass the interfacial conductance between the steel pipe and the refractory was examined. After some adjustments and modifications of the equipment, the test procedures turned out to be well working and easily repeatable.

The test results showed that the received thermal conductivity values were close to the estimates given by the material providers and the steel studs inside the refractory had a notable effect onto the overall heat transfer coefficient of the test tube system. Minor gap formation happened at the interface without studs, which was seen as the increase in the thermal resistance at the interface during the test runs. The obtained values for interfacial conductance cannot be used as such because they vary due to multiple things that cannot be controlled during the installation such as the contact pressure between the layers. Nevertheless, the phenomena of gap formation itself is an important thing to take into account.

In conclusion, a test procedure for the testing of the thermal conductivity of a refractory in a cylindrical system was planned and executed and the procedure worked as it was planned as trustworthy and repeatable test results were obtained. Thus, the equipment can be used also in the future to examine the heat transfer of different masses or other type of cylindrical multi-layer systems.

TIIVISTELMÄ

PERTTI TAPIAINEN:
Lämmönsiirron kokeellinen määrittäminen radiaalisissa suljetuissa systeemeissä
Tampereen teknillinen yliopisto
Diplomityö, 50 sivua
Syyskuu 2016
Diplomi-insinöörin tutkinto, Ympäristö- ja energiatekniikan koulutusohjelma
Pääaine: Voimalaitos- ja polttotekniikka
Tarkastajat: Professori Risto Raiko ja Professori Erkki Levänen

Avainsanat: lämmönjohtuvuus, rajapinta, lämmönsiirto, muurauskerros

Tämän työn tavoitteena oli suunnitella ja toteuttaa helposti toistettavissa oleva tutkimusmenetelmä erilaisten muurausmateriaalien lämmönjohtuvuuden selvittämiseksi. Lisäksi tavoitteena oli tutkia teräsputken ja sitä ympäröivän muurauskerroksen välistä rajapintavastusta, jotta saataisiin parempaa tietoa muurauksen ulkopinnan ja teräsputken sisäpuolen välisestä kokonaislämmönsiirtokertoimesta.

Koelaitteisto koostui eristetystä putkiuunista sekä vedenjakelulaitteistosta, jonka avulla pystyttiin säätämään koekappaleen sisällä kiertävän veden lämpötilaa, painetta ja tilavuusvirtausta. Kolmea eri teräsputkien päälle valettua muurausmassaa testattiin ja yhtä massoista käytettiin myös tapitetussa teräsputkessa, jotta tappien vaikutusta lämmönsiirtoon voitiin testata. Muurauskerroksen lämmönjohtumisen lisäksi myös rajapinnan lämmönsiirtoa teräsputken ja muurauksen välillä tutkittiin. Muutamien koelaitteiston säätöjen ja muokkauksien jälkeen koejärjestelyt osoittautuivat hyvin toimiviksi sekä helposti toistettaviksi.

Testitulokset osoittivat, että saadut arvot lämmönjohtumisille olivat lähellä materiaalitoimittajan antamia arvioita ja muurauskerroksen sisällä olleilla terästapeilla oli merkittävä vaikutus koekappaleen kokonaislämmönsiirtokertoimeen. Lievää raon muodostumista oli havaittavissa rajapinnassa koekappaleissa, joissa ei ollut tapitusta, mikä näkyi rajapintavastuksen kasvuna testien edetessä. Saatuja arvoja rajapinnan lämmönsiirtokertoimille ei voida käyttää sellaisinaan, koska niihin vaikuttaa moni asennusvaiheessa hallitsematon tekijä kuten pintojenvälinen kontaktipaine. Raon muodostuminen on kuitenkin ilmiönä tärkeä huomioonotettava seikka.

Yhteenvetona todettakoon, että koejärjestely muurausmateriaalien lämmönjohtumisen selvittämiseksi sylinterin muotoisessa systeemissä suunniteltiin sekä toteutettiin ja järjestely todettiin hyvin toimivaksi sen antaessa luotettavia ja toistettavia tuloksia. Täten laitteistoa voidaan käyttää myös jatkossa erilaisten muurausmassojen tai muiden sylinterin muotoisten kappaleiden lämmönsiirron tutkimiseen.

PREFACE

This thesis was written at the Tampere University of Technology (TUT) during the time period from December 2015 to July 2016 at the department of Material Sciences through the funding of Valmet Technologies Oy.

I would like to thank Professor Risto Raiko for helping me especially with the theory of heat transfer. I would also like to thank the ceramic material team of Professor Erkki Levänen and particularly Jussi Silvonen who helped me with material questions and provided some extra hands during the test preparations. From Valmet Technologies Oy I would like to thank especially Pekka Lehtonen and Mikko Uusitalo who both had a huge impact on the project planning even before I began my work and they always answered to my questions without any delays. Other people who had a positive impact on my thesis project were: Tero Luomaharju, Juha Savolainen, Juha Sutinen, Juha Toiminen, Tarmo Toivonen and Ari Varttila.

Through the years of studying at TUT my life has been made a lot more pleasant and interesting by all the friends that I have made in different groups and for that I would like to thank especially Ympäristöteekkarikilta, but also Kiltaneuvosto 2012, NääsPeksi, Tampereen Teekkarien Soitannollinen Seura and Yrityspäivät. All of these organizations have given me many wonderful memories. My studies abroad at Universidad Politécnica de Valencia were also an eye-opening experience thanks to all the great people I met there. Thank you also to TUT and its student council for making these seven years the best a university student could have!

Last but not least I would like to thank my mother for supporting me through these 20 years of studying. Now it is time for me to put the knowledge into use!

TABLE OF CONTENTS

LIST OF SYMBOLS AND ABBREVIATIONS

LC	Low cement
SiC	Silicon carbide
TUT	Tampere University of Technology
A	surface area [m^2]
A_c	cross-sectional area [m^2]
B	temperature distribution variable
c_p	specific heat capacity [J/kgK]
D	diameter [m]
F	Hottel factor for thermal radition
F_s	shape factor
f	friction factor
Gr	Grashof number
h_c	convective heat transfer coefficient [W/m^2K]
h_i	interfacial conductance [W/m^2K]
h_r	radiative heat transfer coefficient [W/m^2K]
k	thermal conductivity [W/mK]
L	length [m]
$\dot{m}$	mass flow [kg/s]
Nu	Nusselt number
P	perimeter [m]
Pr	Prandtl number
$\dot{Q}$	heat flow [W]
q	heat flux [W/m^2]
R	thermal resistance [K/W]
Ra	Rayleigh number
Re	Reynolds number
r	radius [m]
T	temperature [K]
$U_{A,out}$	overall heat transfer coefficient by the outside surface [W/m^2K]
V	mean velocity [m/s]
x	coordinate in the flow direction [m]
β	volumetric coefficient of thermal expansion [1/K]
ε	emissivity
η_f	fin efficiency
η_t	total surface efficiency
μ	dynamic viscosity [kg/ms]
ν	kinematic viscosity [m^2/s]
ρ	density [kg/m^3]
σ	Stefan-Boltzmann constant
χ	fin parameter

1. INTRODUCTION

Refractories play a significant role in the heat transfer in power plants. Their main purpose is to protect the pipes transporting heated water or steam, but while doing so, they also act as insulators, which is an un-wanted effect in order to have the best possible efficiency from the fuel used in the power plant. This is why the thermal conductivity of a refractory material is an essential piece of information a designer should know.

The refractory suppliers provide values for the thermal conductivity of the refractory materials, but they are often closer to estimates than trustworthy test results or calculations. In addition to the knowledge of the actual refractory material, there are several other factors that influence the heat transfer. The most significant part comes from the area between the pipe and the refractory, because there are always resistances to heat transfer when two different surfaces meet each other. Different reasons for the resistance of heat transfer in the interface are caused by possible air gaps between the surfaces, rust, paint or other coatings on the pipe, and the fact that material surfaces are never totally smooth, leading to decreased contact area for the heat to flow.

This is why the whole heat transfer system with the pipe and the refractory material on top of it has to be examined to receive better information of the total heat transfer coefficient from the surroundings to the inside contents of the pipe. The objective of this study is to design and conduct a test method that can be easily replicated to find out the conductivities of different refractory materials and also to investigate the interfacial resistances.

In this study a fully insulated electrical heater oven will work as the source of heat and the produced heat will be absorbed by a flow of water inside a pipe covered by a casted refractory material. Temperatures at different points of interest as well as the volume flow of the water will be measured to determine the heat flow in the system and furthermore the conductivity of the refractory material and the interfacial resistance. The received values for the conductivities of different materials will be compared to the values given by the material providers.

The obtained test results can be used in the process designing of a steam power plant to make the energy balance calculations more accurate and trustworthy. This will also help to trace possible problematic points where un-wanted thermal resistance exists and to give some knowledge of the behavior of different refractory masses or layer structures.

2. LITERATURE SURVEY OF THE HEAT TRANSFER IN MULTI-LAYERED CONSTRUCTIONS

Heat is a form of energy that can be transferred in three different methods, which are: conduction, convection and radiation. In a molecular level, when a substance has a higher level of energy, or in this case heat energy, it starts to vibrate and while vibrating, it hits molecules next it causing them to vibrate too. This rise of vibration is on a macroscopic level seen as rising temperature as the vibration spreads like a chain reaction from one molecule to another in the same block of material. Ergo, in heat conduction only the heat energy is transferred, when the molecules themselves remain in place.

The heat flow $\dot{Q}$ [W] depends on the distance between the two points of a fragment, or simply the length L [m], and the area A [m^2] of the examined fragment, which in this case could be a plate. The heat also tries to even out as fast as it can, which means the greater temperature difference ΔT [K] of the different ends of the fragment is, the greater the heat transfer is. The final thing that that has an effect on the heat transfer is the material itself. This material based variable k [W/m K] is called the thermal conductivity, which in addition to the change of substance varies slightly also with the change of temperature. The heat flow can be calculated from these variables mentioned above, using equation 3 conducted from the Fourier's law of heat conduction [1]:

$$q = \frac{\dot{Q}}{A} = -k\frac{dT}{dx} \quad , \tag{1}$$

where q [W/m^2] is the heat flux or heat flow per unit area perpendicular to the flow direction and x [m] is the coordinate in the flow direction. Because the variables are separable, integrating across the fragment leads to:

$$\frac{\dot{Q}}{A}\int_0^L dx = -\int_{T_1}^{T_2} k dT \tag{2}$$

When $\dot{Q}$, A and k are considered as constants towards their integrators, the equation for heat conduction across a wall becomes:

$$\dot{Q} = \frac{kA}{L}(T_1 - T_2) \, , \tag{3}$$

where the factor L/kA can be viewed as the thermal resistance for conduction R_{cond} [K/W] when using the electrical resistance analogy, where in comparison to the Ohm's law, $I = U/R_{electrical}$, the equation for heat flow is $\dot{Q} = \Delta T/R_{thermal}$.

The heat convection differs from the heat conduction in a way that instead of just exchanging energy to neighboring molecules, the particles carrying energy actually move,

which means convection doesn't take place inside solid materials. The term heat convection is used to describe the heat exchange between surfaces and fluids. The heat exchanged by convection can be calculated with the following equation often also called as the Newton's law of cooling [1]:

$$\dot{Q} = h_c A \Delta T, \tag{4}$$

where h_c is the convective heat transfer coefficient [W/m^2 K] and ΔT is the temperature difference of the fluid T_e and the surface T_s. The thermal resistance for surface with convection is $R_{conv} = 1/h_c A$.

The third method of heat transfer is thermal radiation. Every object sends electromagnetic waves or photons, which possess energy that is transferred to another object when meeting its surface. The basic equation for heat flow in thermal radiation from surface 1 to surface 2 is presented below [2]:

$$\dot{Q}_{12} = A_1 F_{12} (\sigma T_1^4 - \sigma T_2^4), \tag{5}$$

where A_1 is the area of the radiating body, F_{12} is a factor, which includes the emissivity, shape and size of the two surfaces and it is often called as the Hottel factor and it is defined from the sender to the receiver, σ is the Stefan-Boltzmann constant, which has a value of 5,670 × 10^{-8} W/m^2 K^4 [3], and T_1 and T_2 are the temperatures of the sender and the receiver, respectively. The material surface properties have a huge impact on the amount of heat transferred from one surface to another and that is why the Hottel factor is used. It signifies the share of the radiation the receiving body gets from the radiator and it is a function of the surface areas and the emissivities, ε, of the two surfaces. The emissivity of a surface signifies the proportion of energy it can emit compared to its full potential, meaning for real or "grey" surfaces: $0 < \varepsilon < 1$. If there is a need for the radiative heat transfer coefficient h_r, it can be calculated from an equation similar to equation 4, when the amount of heat flow is known. The thermal resistance for a surface with both convection and radiation is calculated as

$$R_{conv,rad} = \frac{1}{A(h_c + h_r)} \tag{6}$$

If a system has heat transfer in all the three forms the overall heat transfer coefficient $U_{A,out}$ [W/m^2 K] can be calculated by summing the resistances in the thermal network in the following way:

$$\frac{1}{AU_{A,out}} = \sum_{i=1}^{n} R_i \tag{7}$$

where R_i represents the different thermal resistances of either heat conduction, convection or radiation in the thermal network. The overall heat transfer coefficient in this study is calculated with the outside layer's surface area of the studied system. Because the amount

of transferred heat is a constant in all the layers of a system, the total amount of heat transferred through the whole system can be calculated with the equation [1]:

$$\dot{Q} = U_{A,out} A \Delta T \,, \tag{8}$$

where ΔT is the temperature difference between the outside and the inside layers of the system.

2.1 Hollow cylindrical systems

This study concentrates on a cylindrical composite tube system shown in the figure 1. The tube is inside an insulated furnace, which means the theory of heat transfer is slightly different from the basic formulas given as examples in the first part of chapter 2. The main difference comes from the cylindrical shape where the temperature is a function of the radial coordinate *r* [m], instead of the length *L* in the case of a plane wall. This also leads to change in the area when the *r* changes since the heat transfer area for cylinder is $A = 2\pi rL$, where *L* is the length of the cylinder. When the radius increases, the area of heat transfer also increases. The experiments in this study are made in steady state conditions, which means time isn't a variable in the calculations.

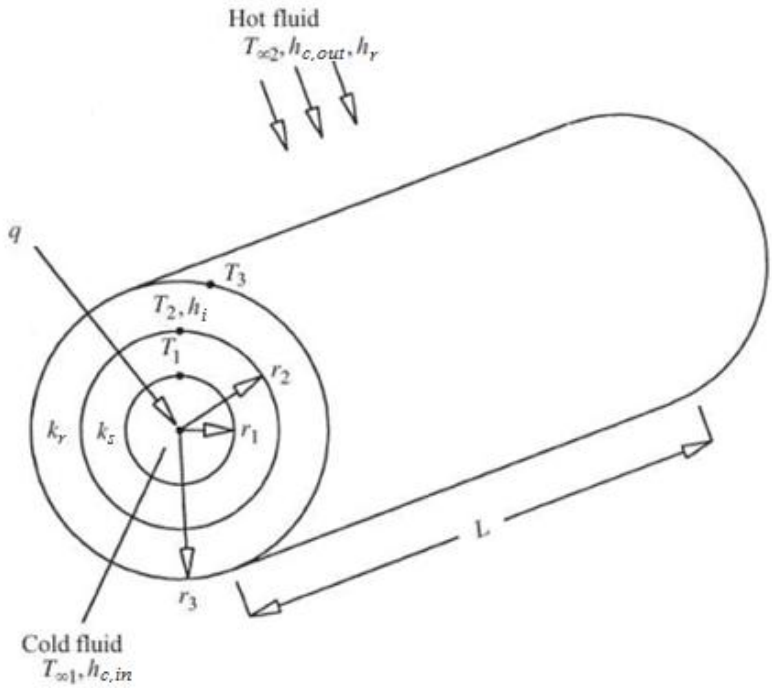

Figure 1. *Composite hollow cylinder with boundary temperatures, convective and radiative heat transfer coefficients, and thermal conductivities with the subscripts r for refractory and s for steel pipe.* [4]

The heat produced in the furnace is transferred into a flow of water inside the tube. The amount of the heat received by the water can be calculated with the equation [1]:

$$\dot{Q} = \dot{m} c_p (T_{out} - T_{in}) \,, \tag{9}$$

where $\dot{m}$ [kg/s] is the mass flow of fluid, c_p [J/kg K] is the fluid specific heat capacity and T_{out} and T_{in} are the fluid temperatures at the outlet and inlet of the studied part.

The temperature distribution inside a cylinder can be derived from the Laplace's equation for cylindrical coordinates in steady state conditions [5]

$$\nabla^2 T = \frac{1}{r}\frac{\partial}{\partial r}\left(r\frac{\partial T}{\partial r}\right) + \frac{1}{r^2}\frac{\partial^2 T}{\partial \Phi^2} + \frac{\partial^2 T}{\partial z^2} = 0 \,, \tag{10}$$

which in this case, when the temperature distribution is considered constant longitudinally and angularly, reduces to one dimensional form:

$$\frac{d^2 T}{dr^2} + \frac{1}{r}\frac{dT}{dr} = 0 \tag{11}$$

The equation 11 has the solution [6]

$$T = B \ln r + C \tag{12}$$

The boundary conditions are:

$$T = T_1 \text{ at } r = r_1 \quad \text{and} \quad T = T_2 \text{ at } r = r_2 \tag{13}$$

and the arbitrary constants B and C in the equation 12 are [6]:

$$B = \frac{T_2 - T_1}{\ln(r_2/r_1)} \quad \text{and} \quad C = T_1 - \frac{\ln r_1 (T_2 - T_1}{\ln(r_2/r_1)} \tag{14}$$

This leads to logarithmic temperature distribution through the cylinder wall and it is given by

$$T = T_1 + \ln\left(\frac{r}{r_1}\right)\frac{T_2 - T_1}{\ln(r_2/r_1)} \tag{15}$$

The equation for heat conduction across a cylindrical shell can be conducted using Fourier's law [6] from the equation 1 and replacing *dx* with *dr* for the cylindrical coordinate it becomes:

$$q = \frac{\dot{Q}}{A} = \frac{\dot{Q}}{2\pi r L} = -k\frac{dT}{dr} \tag{16}$$

Because the variables are separable, integrating across the fragment leads to:

$$\frac{\dot{Q}}{2\pi L}\int_{r_1}^{r_2}\frac{1}{r}dr = -\int_{T_1}^{T_2} k dT \tag{17}$$

When $\dot{Q}$, L and k are considered as constants towards their integrators, the equation for heat conduction across the section of a cylinder becomes:

$$\dot{Q} = \frac{2\pi kL(T_1 - T_2)}{ln(r_2/r_1)} \tag{18}$$

where r_1 and r_2 are the inner and outer radii an T_1 and T_2 are their temperatures, respectively. When calculating with the electrical resistance analogy, the thermal resistance for a cylindrical shell is

$$R_{cond} = \frac{\ln(r_2/r_1)}{2\pi kL} \tag{19}$$

From the equation 18, the conductivity of a material can be calculated in the following way if all the other values are known:

$$k = \frac{\dot{Q}\ln(r_2/r_1)}{2\pi L(T_1 - T_2)} \tag{20}$$

The value given by the equation 20 is the mean thermal conductivity of the chosen interval. In reality, the conductivity varies with temperature changes [7]. Figure 2 presents an example of the irregular temperature dependence of thermal conductivity.

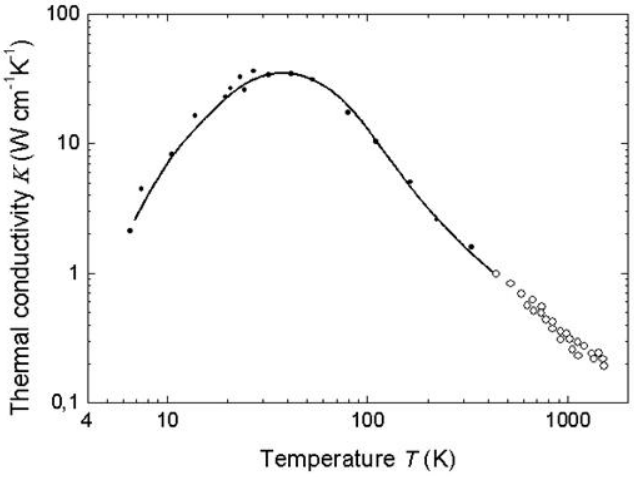

Figure 2. *Temperature dependence of thermal conductivity for high purity Silicon. [7]*

Because the thermal conductivity varies with the temperature, a fitting for the thermal conductivity curve is needed for more accurate results. A good method for curve fitting is a polynomial function [8]:

$$k(T) = \sum_{i=0}^{n} a_i T^i = a_0 + a_1 T + a_2 T^2 + a_3 T^3 + \cdots + a_n T^n \tag{21}$$

The constants a_0 to a_n can be solved when the thermal conductivities at $n+1$ amount of temperatures are known.

The theory and equations for heat transfer through heat convection and thermal radiation for cylindrical shells are similar to those presented earlier in the chapter 2, because these

types of heat transfer only have an effect on the surface of the material, which means the heat transfer area in the equations 4 and 5 already include the knowledge of the radius, because $A = 2\pi rL$.

The calculation of the convective heat transfer coefficient is relatively complicated. It can be calculated with the help of a dimensionless Nusselt number *Nu*, but the complexity comes from the fact that there are several different formulas to calculate the Nusselt number depending on the situation in hand. In a tube the Nusselt number is connected to the convective heat transfer coefficient as follows [1]:

$$h_c = \frac{Nu_D k}{D}, \tag{22}$$

where *D* is the inside diameter of the pipe. In order to calculate the Nusselt number, the value of Reynolds number *Re* has to be known. Reynolds number for a tube is defined as follows [1]:

$$Re_D = \frac{VD}{\nu}, \tag{23}$$

where *V* [m/s] is the mean velocity of the flowing fluid and ν [m^2/s] is the kinematic viscosity. The value of the Reynolds number reveals if the flow is laminar or turbulent. The flow starts to turn turbulent in the region of $Re_D \approx 2300$ although it is only until the $Re_D > 10^4$ that the flow is considered fully turbulent. For $3000 < Re_D < 10^6$ the Nusselt number for internal turbulent flow in a pipe can be calculated using the Gnielinski's formula [1]:

$$Nu_D = \frac{(f/8)(Re_D - 1000)Pr}{1 + 12.7(f/8)^{1/2}(Pr^{2/3} - 1)}, \tag{24}$$

where *Pr* is the Prandtl and number f is the friction factor, which when using the Gnieleski's formula has to be calculated with Petukhov's formula [1]:

$$f = (0.790\, ln(Re_d) - 1.64)^{-2} \tag{25}$$

The Prandtl number is defined as [1]:

$$\mathrm{Pr} = \frac{c_p \mu}{k}, \tag{26}$$

where μ [kg/m s] is the dynamic viscosity, which is tied to the kinematic viscosity by the density ρ [kg/m^3] of the fluid $\mu = \nu\rho$. The Nusselt number calculated with the equation 24 doesn't include the entrance effect, which means that close to the entrance the flow isn't fully turbulent yet, even if the Reynolds number would suggest it. This results to the average Nusselt number to be bigger than the calculated one. The table 1 shows correlations for Nusselt number ratios with the distance from the end of the pipe for different entrance configurations.

Table 1. *The ratio of average Nusselts number to the fully developed value,* $\overline{Nu}/Nu_\infty$*, for Pr close to unity* [1].

	Distance from pipe entrance in diameters									
Entrance configuration	2	4	6	8	10	20	40	80	160	320
Long calming section	1.49	1.34	1.26	1.21	1.17	1.10	1.06	1.03	1.01	1.01
Open end, 90° edge	2.36	1.95	1.73	1.60	1.54	1.32	1.18	1.09	1.05	1.02
90° elbow	2.15	1.86	1.68	1.57	1.49	1.32	1.18	1.09	1.05	1.02
Tee (confluence)	1.77	1.56	1.44	1.36	1.31	1.19	1.10	1.06	1.03	1.01
90° round bend	1.63	1.44	1.34	1.28	1.24	1.16	1.10	1.05	1.03	1.01
180° return bend	1.54	1.37	1.28	1.23	1.19	1.12	1.08	1.04	1.02	1.01

Table 1 shows that after the distance of about 40 times the pipe diameter, the flow begins to be fully developed.

The convective heat transfer coefficient in the case of outside natural flow on a horizontal cylinder is calculated similarly as in the equation 22, but the Nusselt number is calculated with a different equation than in the case of internal flow. To determine if the flow is laminar, Rayleigh number Ra needs to be calculated [1]

$$Ra_D = Gr_D Pr, \tag{27}$$

where Gr_D is the Grashof number, which is defined as [1]

$$Gr_D = \frac{\beta \Delta T g D^3}{\nu^2}, \tag{28}$$

where ΔT is the temperature difference between the surface and the surrounding space, g is the standard gravity with the value of 9.087 m/s^2 and β [K^{-1}] is the volumetric coefficient of thermal expansion, which can be calculated from the mean gas temperature T_g of the fluid surrounding the surface $\beta = 1/T_g$. If $Ra_D \leq 10^9$, the flow is laminar and the correlation of Churchill and Chu [1] for laminar natural convection on a surface of a cylinder can be used to determine the average Nusselt number:

$$\overline{Nu}_D = \frac{0.518 Ra_D^{1/4}}{[1+(0.559/Pr)^{9/16}]^{4/9}}. \tag{29}$$

The proportion of the transferred heat by radiation is defined by the view factor or the radiation transfer factor F and it shouldn't be confused with the shape factor F_s. The view factor from surface 1 to surface 2 is calculated as follows [1]:

$$F_{12} = \frac{1}{\frac{1-\varepsilon_1}{\varepsilon_1 A_1} + \frac{1}{A_1 F_{s12}} + \frac{1-\varepsilon_2}{\varepsilon_2 A_2}}, \tag{30}$$

where the subscript 1 refers to the surrounding transmitting surface and the subscript 2 refers to inner object's receiving surface. Because the studied cylindrical object is inside

an insulated cylindrical oven, the shape factor $F_{s12} = A_2/A_1$ [1] in the equation 30. With the help of the view factor and the equation 5 the amount of thermal radiation can be calculated.

After determining the thermal conductivities, convective heat transfer coefficients, radiative heat transfer coefficient and the interfacial conductance, the thermal network of the overall heat transfer coefficient from the equation 7 for the system presented in the figure 1 becomes:

$$\frac{1}{AU_{A,out}} = R_{conv,in} + R_{cond,1} + R_{interface} + R_{cond,2} + R_{conv,rad,out} \tag{31}$$

$$\frac{1}{AU_{A,out}} = \frac{1}{2\pi r_1 L h_{c,1}} + \frac{\ln(r_2/r_1)}{2\pi k_1 L} + \frac{1}{2\pi r_2 L h_i} + \frac{\ln(r_3/r_2)}{2\pi k_2 L} + \frac{1}{2\pi r_3 L(h_{c,2}+h_r)}, \tag{32}$$

where h_i [W/m^{2}K] is the contact conductance or interfacial conductance, which will be discussed more thoroughly in the following section in the chapter 2.2. If the overall heat transfer coefficient is wanted, it is calculated in this study with the outside layer's surface area $A = 2\pi r_3 L$, from the figure 1.

2.2 Contact resistance between the layers

In an ideal case, two materials that are in contact with each other don't have any gap between their surfaces, which mean their surface temperatures are the same. In the real world, there are always small gaps, which lead to imperfect heat transfer in the contact area. This so called contact resistance $R_{t,c}$ [K/W] depends on several factors including surface roughness, surface materials, contact pressure and interstitial conditions such as the substance in the gaps as well as the temperature [9]. Due to the uneven surfaces of real materials, the heat flow has to squeeze itself through the narrow points, where the meeting surfaces touch each other as in the figure 3, which shows also another reason for the complexity of the contact resistance, which is that the heat is also transferred by radiation and conduction in the gaps [1].

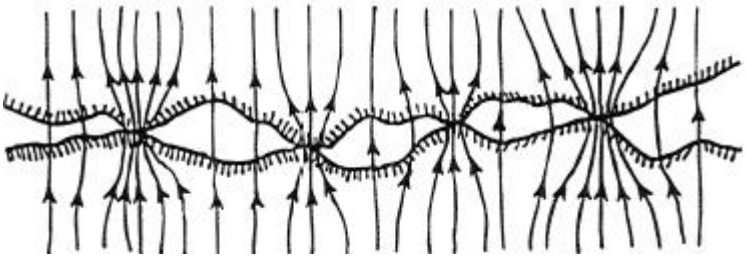

Figure 3. *Closer look at an interface of two materials* [9].

The contact resistance is often expressed as a thermal contact conductance or an interfacial conductance h_i [1]. The interfacial conductance can be defined from Newton's law

of cooling similarly as in the equation 4 where h_i is used in the place of h_c and the ΔT_i is the temperature difference of the two contacting surfaces, which leads to the definition of interfacial conductance to be [4]:

$$h_i = \frac{\dot{Q}}{A\Delta T_i} \tag{33}$$

There exists some data for interfacial conductances, but since the values depend on numerous factors, the data is quite unreliable and incomplete. Typical interfacial conductances are presented in the table 2.

Table 2. *Typical values of interfacial conductances* [1].

Contacting faces	Interfacial conductance h_i [W/m^2 K]
Ceramic-ceramic	500 – 3000
Ceramic-metals	1500 – 8500
Stainless steel-stainless steel	1700 – 3700
Aluminum-aluminum	2200 – 12000
Stainless steel-aluminum	3000 – 4500
Copper-copper	10000 – 25000

As the data in the table 2 shows, the values for interfacial conductance vary so much, that they cannot be used as such, but at least they give an idea of the ranges they should be in and they also suggest that the smoother the surfaces are and the higher conductivity a certain material has, the better they conduct heat in the interface.

There are also some equations [10] to determine the interfacial conductance, but in order to calculate it, one must first measure multiple factors such as the temperatures, surface roughnesses, the shape of the gaps and the contact pressure, which means measuring the interfacial conductance itself is a better solution.

2.3 Effect of construction elements crossing the layers

Some of the cases in this study include steel tubes with steel studs used as anchors for the casted refractory materials. The studs will increase the surface area of the steel tube causing increase in the amount of heat transfer in the system. However, the growth of heat isn't proportional to the added area, even if the product of h_cA increases with the area, because of the temperature gradients along the studs. These studs behave similar to theoretical cooling fins except that in this study the fins are actually heating up the steel tubes, not cooling them down as the cooling fins would normally do. Because the temperature at the end of the studs is closer to the temperature of the surrounding area, the average temperature difference (T_s - T_e) between the studded tube and its surrounding area is smaller than in the case of a bare tube. This means that in the case of a studded tube the

term h_cA for the studded part has to be replaced with the term $h_cA\eta_f$, where η_f is the fin efficiency $0 < \eta_f < 1$. [1]

The fin efficiency can be calculated with the knowledge of the perimeter P and the length L of the fin or a stud, when h_c and the temperature difference between the base of the fin and the surroundings (T_B - T_e) are known. A compact form for the equation is

$$\eta_f = \frac{\tanh \chi}{\chi}, \tag{34}$$

where the dimensionless fin parameter χ = BL for a pin fin. The symbol B is used to simplify the conduction of the equation 34 and its definition is

$$B = \sqrt{(h_c P)/(kA_c)}, \tag{35}$$

where P [m] is the perimeter of the fin and A_c [m^2] is its cross-sectional area. [1]

The amount of heat transfer from a single pin fin can be calculated using the following equation [1]:

$$\dot{Q} = \frac{(T_B - T_e)}{1/[(h_c P/B)\tanh\ BL]}, \tag{36}$$

which means the thermal resistance of a pin fin is

$$R_{fin} = \frac{1}{(h_c P/B)\tanh(BL)} = \frac{1}{h_c P L \eta_f}. \tag{37}$$

The total surface efficiency η_t of a surface with fins is of course greater than the fin efficiency, since the efficiency for the unfinned are is 100 %. The total surface efficiency can be calculated as follows [1]:

$$\eta_t = 1 - \frac{A_f(1-\eta_f)}{A}, \tag{38}$$

where A_f is the fin surface area and A is the total heat transfer area including the fin surface area. After obtaining the total surface efficiency for a finned surface, its thermal resistance can be calculated with the following equation [1]:

$$R = \frac{1}{h_c A \eta_t}, \tag{39}$$

which can be later used to calculate the amount of heat flow through the surface layer of a tube.

2.4 Experimental apparatus in publications by others

Similar kind of radial heat flow apparatus as the one utilized in this study was used by Madshuana and Litvak. The main differences in the system were that the temperatures weren't as high as in this study because the heating up was done with hot liquid cycle, which meant the system was similar to a conventional heat exchanger where the hot liquid was running through the insides of the test tube and the cold liquid flowed over the surroundings of the tube. This also meant that there wasn't a gas phase as in this study and in the real power plants. Figure 4 shows the apparatus. [11]

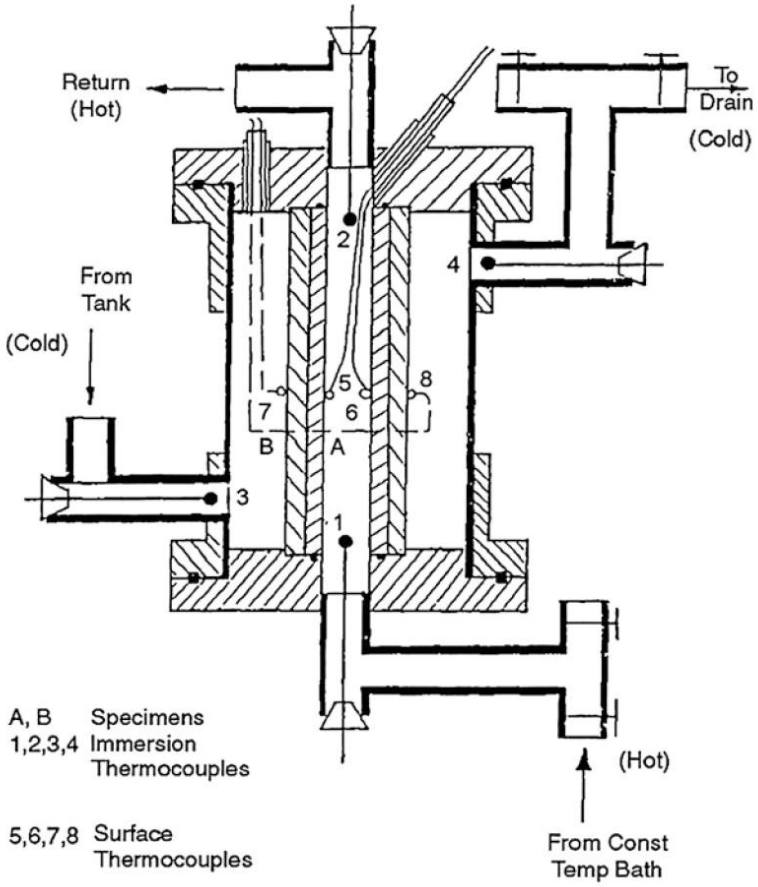

Figure 4. *Radial heat flow apparatus of Madhusuana and Litvak* [11].

The test tube consisted of two different materials, one being inside the other coaxially, and the thermocouples were attached only on the reachable surfaces of the two materials. This meant that the final result for thermal conductivity was an average value for the whole system's heat transfer, consisting of the two material's thermal conductivities and the thermal contact conductance at the interface between the surfaces of the two specimen. The apparatus was used to measure thermal contact conductance between two specimens whose thermal conductance were already known. [11]

More common experimental apparatus type for thermal conductivity measurements is presented in the figures 5 and 6. The apparatus can only measure small items and the used temperatures aren't usually very high as they are often close to room temperature.

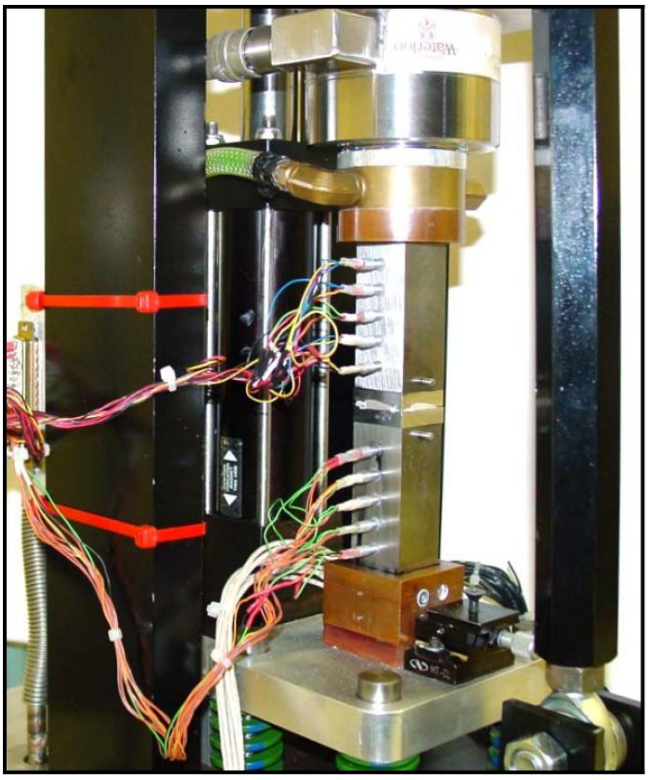

Figure 5. *Small scale thermal conductivity and contact resistance measurement apparatus* [12].

A small stable heat flux is produced by electrical heating. The heat flux goes through the flux meters that have metal blocks in between of them. The metal blocks have also temperature measurement sensors to find out the temperature gradients. The actual experimented block is placed between the metal blocks and in this study it was an adhesive material, but also plates made of metals, ceramics or plastics can be used. This procedure can also be used to measure contact resistances, if the conductance of the experimented block is known. The order of the blocks is presented in the figure 6. [12]

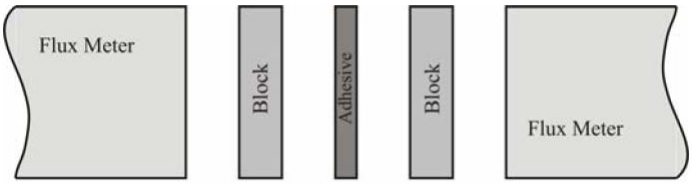

Figure 6. *The blocks in the measurement system* [12].

The figures 5 and 6 show that the material between these two blocks must be very thin, but a similar equipment could be used to measure just the contact conductance by leaving the material in the middle, which is in this case is an adhesive, out from the interface.

3. MATERIAL PROPERTIES

The materials for the refractory castings in this study were casted at AG Port Oy. The first mass was conventional low cement (LC) mass and it was used in the cases 2 and 3. The second mass used for the case 4 was an insulating mass and the third mass was a better heat conducting silicon carbide (SiC) mass and it was used in the case 5. The thermal conductivities of the different masses according to the material provider are presented below in the table 3.

Table 3. *The conductivities of the used refractory material masses* [13][14][15].

	LC mass	Insulating mass	SiC mass
Thermal conductivity, k_r [W/mK]	1.1	0.2	5.8

In addition to the chemical composition of a mass, the porosity has a great effect on the heat conduction. The porosities of LC and SiC masses are relatively low, whereas the porosity of insulating mass is so high that it cannot be evaluated without measurements. When the size and the amount of pores increase, the conductivity of the mass decreases due to the low heat transfer through gases. This is why insulating masses have high porosity. The insulating effect of pores does however decrease a bit when higher temperatures are reached due to the thermal radiation, which starts to have an impact on the heat transfer through the pores at high temperatures.

The estimates on the table 3 will be compared to the received values from the tests later in this study. The thermal conductivity of a refractory mass isn't easily estimated because there are multiple factors that have an effect on it such as the way it is installed, the amount of water that is used during the preparation of the mass for installation, the way it is mixed and the contact pressure it has against the material it is attached to, which can be for example a steel pipe.

The steel pipes in this study are made of 16Mo3 steel and their thermal conductivities at different temperatures are presented in the following table 4.

Table 4. *The thermal conductivity of 16Mo3 steel at different temperatures* [16].

Temperature, T [°C]	Thermal conductivity, k_s [W/mK]
20	48.5
300	43.1
400	39.9
500	38.6

The steel plates at the oven walls are made of 253 MA stainless steel (AISI 312) and its emissivity is about 0.26 [1]. The emissivity will change drastically if oxidation occurs, which means it is impossible to give an exact value for it. The emissivity for white refractory cement is approximately 0.90 [17].

4. COMMISSIONING OF A NEW TEST RIG

The test rig in this study was planned and made for the purpose of these experiments and it consists of three main parts: an electrical oven, a water distribution system and test tubes. The data is gathered from all of these different parts and transferred to a computer using a data logger device. Both the oven and water distribution system are custom made by different companies. The test setup is presented below in the figure 7.

Figure 7. *The test setup.*

The test setup and lay-out presented in the figure 7 shows all the components used in this study. The testing room has to be damp-proof and connections to cooling water cycle and to the municipal water supply are also needed. The room also needs to have three-phase electric power connections for the oven.

4.1 Assembly of the system

The test system in this study consists of a cylindrical electrical oven provided by Oy Resiterm Ab and a water distribution system from Hytar Oy Water Hydraulics.

The oven is well insulated and considered a closed system with the exception of two small holes in the ends of the oven, where the test tubes go through. The oven has two electrical

heaters, one on the bottom of the oven and the other on top on the lid. The oven has a total heating power of 6 kW with 230 V. The heat distribution from the two heaters is evened out by cylindrical electrically zincified 253 MA stainless steel plates placed on the inside of the oven next to the heaters. From the inside, the oven is cylindrical with a length of 600 mm and a diameter of 200 mm. The outside measures are: length 850 mm, width 680 mm and height 1220 mm. The oven is insulated with 50 mm thick mineral wool plates and the ends have also an extra 50 mm insulating wool layer. The oven is presented below in the figure 8.

Figure 8. *The oven with its lid opened.*

The temperature of the heater is controlled by an electronic controller, OMRON E5C, which also works as a digital display of the temperature. The temperature of the oven is measured with a K-type thermocouple close to the steel plate surface inside the oven and the temperature is brought to another OMRON E5C controller which has also an output

line for the data to be transferred with a current signal to an Agilent analog data logger connected to a computer. The temperature of the hot steel plate is also measured with a K-type thermocouple and brought to the data logger. The controller unit is shown in the following figure 9.

Figure 9. *The oven controller unit.*

The water distribution system provides the water into the test tubes placed inside the oven. The system consists of a pump, a heat exchanger and a controlling system and it is presented in the figures 10 and 11. The systems maximum pressure is 5 bar and it produces a water flow up to 15 liters per minute. The water for the test cycle is brought from the mains of TUT and the system is filled up to a pressure of 0.8 bar which is the pressure level where the pump can be started. The test cycle heats up the water and the temperature of the water is controlled with the help of a heat exchanger to cool the temperature down to the wanted temperature. The cooling water for the heat exchanger is brought from the cooling water pipes of TUT. The velocity of the water flow is controlled with a valve on top of the system and the temperature of the water is controlled with a thermostat. The pressure, the amount of flow and the inlet and outlet water temperatures are observed on the top of the system. The inlet and outlet water temperatures in the test tubes are measured with sealed thermocouple rods slid from the connection points of the test tubes and the water hoses and kept away from the inside walls of the tubes by small steel studs made from screws. The water hoses are connected to the test tubes with a 90° angle to make the temperature measurements possible. The data of the temperature measurements as well as the data of the volume flow rates are gathered to the data logger with current signals that are modified to voltages with a 250 Ω resistor before connected to the data logger.

Figure 10. *The water distribution system.*

The figure 10 presents the water distribution system and its connecting water hoses. The big ones on the top are the ones that bring the water into the test tube and back. On the bottom of the picture are the system's emptying and filling hoses that have also controllable valves with them, the safety output valve's hose in case of too high pressure level and the input and output hose connections for the heat exchanger's cooling water circulation. The volume flow level of the water in the test cycle can be controlled with the valve on lid of the system. The following figure 11 shows the water distribution system from the inside.

Figure 11. *The parts of the water distribution system.*

The insides of the water distribution system reveal the essential parts for the water cycle controlling. On the bottom left of the figure 11 is the heat exchanger, which functioning level can be controlled with the black thermostat. On the left top corner is the volume flow meter. The blue pump and its pressure tank can be seen on the right hand side of the figure 11.

4.2 Description of the test tubes

The test tubes are 1500 mm long steel tubes with an outer diameter of 38 mm and a wall thickness of 5 mm. Some of the tubes have also steel studs on them which are 50 mm long with a diameter of 8 mm. Whether a tube has these studs, will be explained in the chapter 5 where the different cases are opened one by one. If the test tube has studs, it has 23 rows of them each row having 6 studs at even 60 degree differences, which means the total number of studs is 138.

Thermocouples are installed to the test tubes to receive temperature data. All of the thermocouples are type K. Thin thermocouple wires are welded onto the surface of the steel pipes and in case the pipes have studs, more wires are welded also at the base and the tip of the studs. Thick 3 mm thermocouple rods are attached to the pipe and bended radially with the shape of a gentle letter Z to distances of 5 mm, 25 mm and 45 mm from the

surface of the steel pipe to receive information of the temperature distribution inside the casted refractory material, which is going to be 55 mm. The distances of the thermocouple attachments are presented in the figure 12.

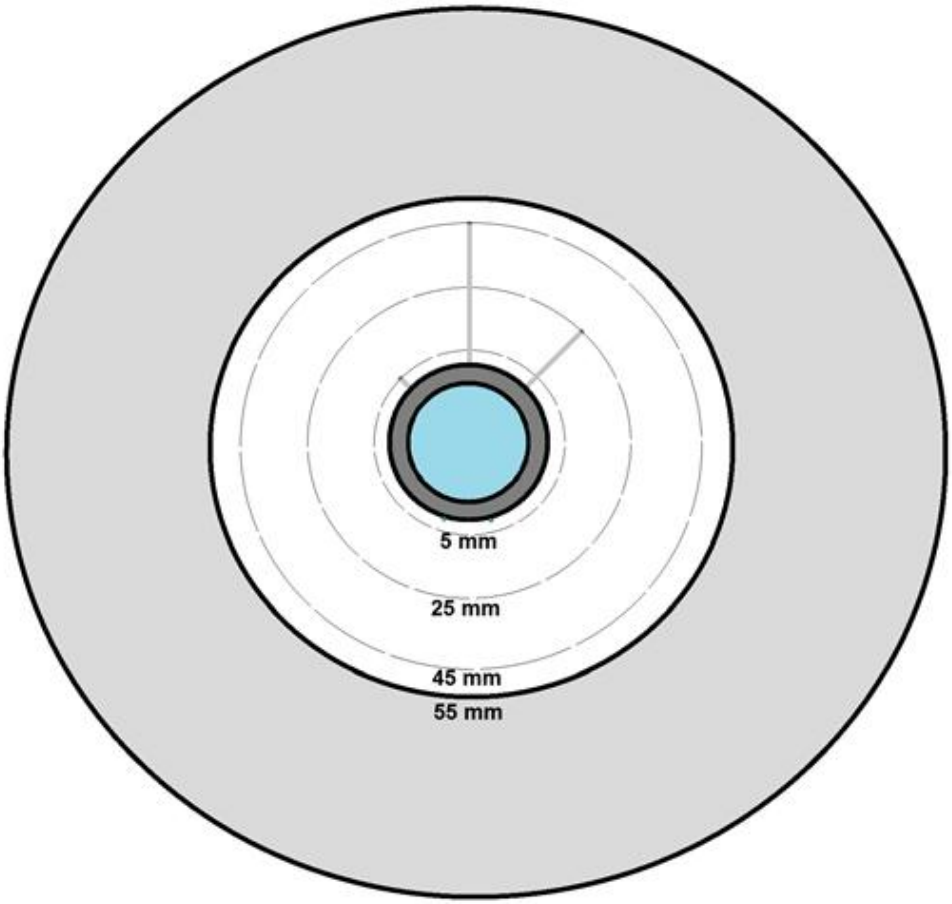

Figure 12. *The thermocouple attachments (gray poles) inside a refractory (white) and their distances from the surface of the steel pipe (dark gray). The thermocouple wires (small green dots) are attached onto the steel pipe. The (light gray) area surrounding the refractory is air inside the cylindrical oven.*

The thermocouple rods are attached so that they move along the pipe longitudinally at a constant distance from the pipe to reduce the effect of their own conduction to disturb the actual temperature levels inside the refractory as it is advised to do [18]. The thermocouple rods were attached by hose clamps after bending them correctly. The following figure 13 presents the welding equipment used in connecting the thin thermocouple wires onto the surface of the steel pipe.

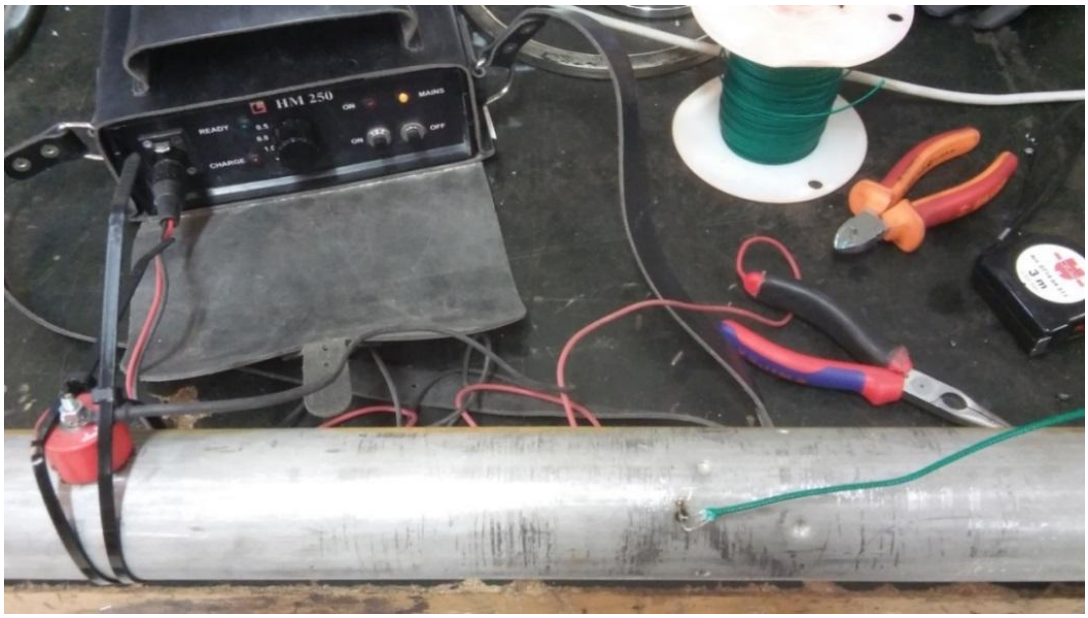

Figure 13. *Welding equipment and a test tube under construction.*

All of the wires were connected longitudinally at the same distance from the end of the pipe in the middle of it. The welding was done with an electrofusion welding equipment. Readymade thermocouple installed steel pipes are presented in the figures 14, 15, 16 and 17.

Figure 14. *A test tube after the thermocouples have been connected.*

Figure 14 shows a test tube without studs after the installation of the thermocouple wires and rods. The same tube is shown closer in the figure 15.

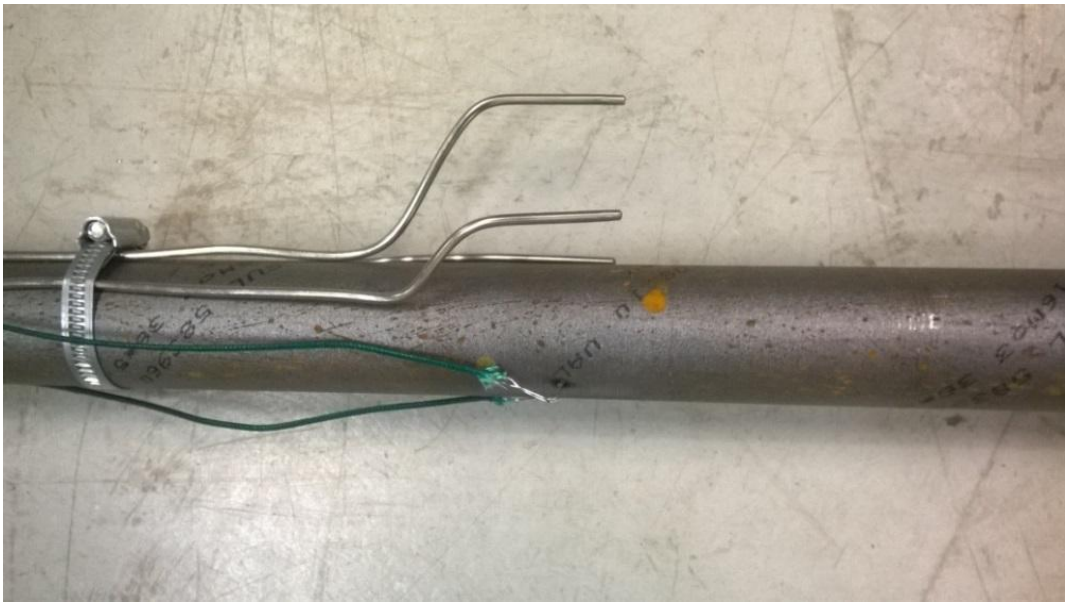

Figure 15. *A closer look at the test tube and its connected thermocouples.*

The thicker thermocouple rods were bent to the wanted distances and longitudinally at the same level. They were however placed at different places angularly in order to decrease the effect of them to disturb each other. The following figure 16 presents a test tube with steel studs installed on the pipe to act as anchors holding the refractory at its place.

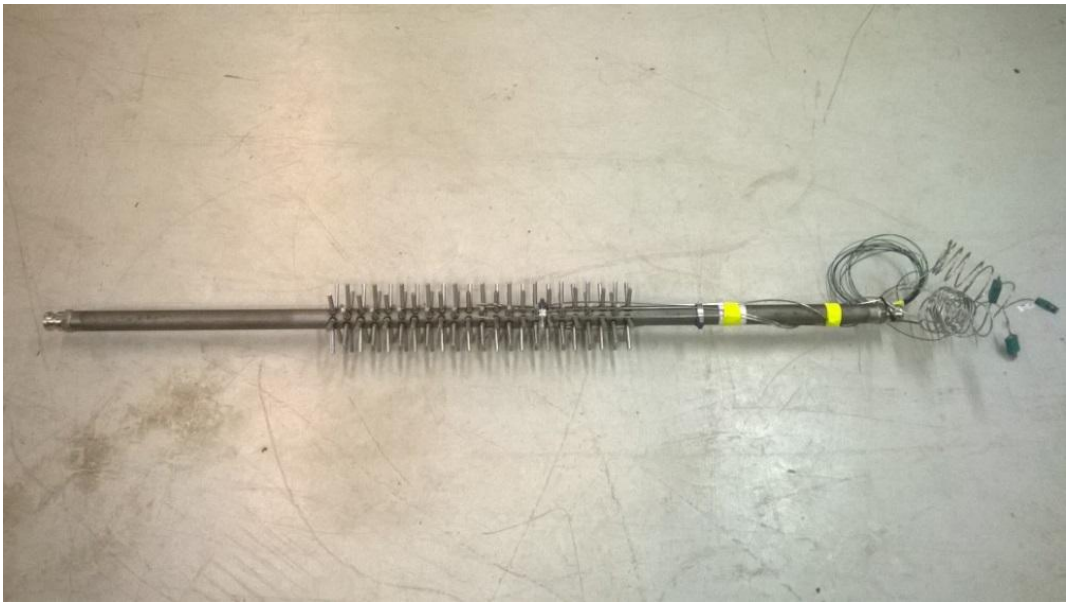

Figure 16. *A test tube with studs after the thermocouples have been connected.*

The thermocouple attachments were done similarly for the studded version as in the case of a pipe without studs. The figure 17 shows a zoomed in view of the attachments.

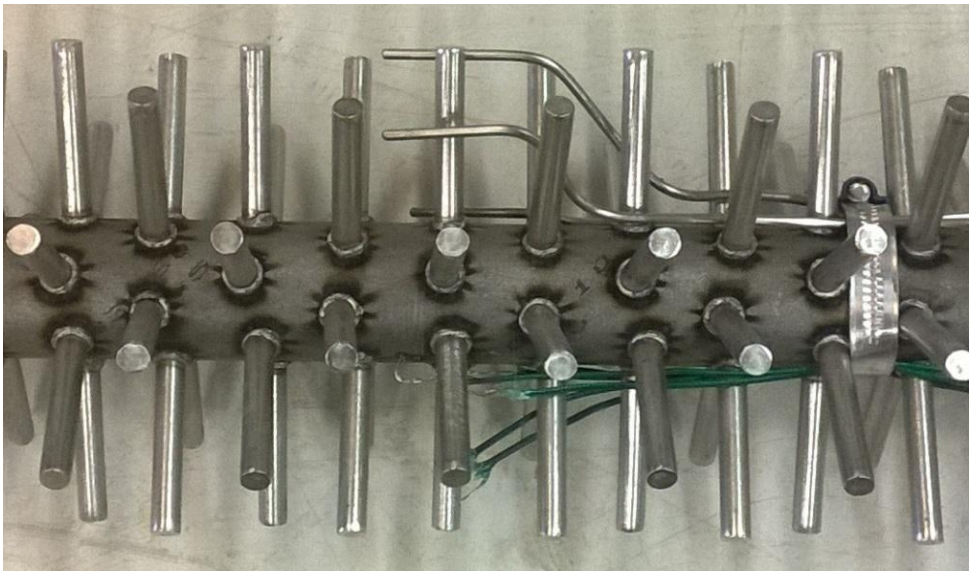

Figure 17. *A closer look at the test tube with studs and thermocouples.*

The refractory cement was casted onto the surroundings of the tubes at AG-Port Oy by the guidelines of the manufacturers of the mass and the casting was done in an area, which was about 600 mm long. The casting was 55 mm thick. This meant the whole steel tube with the casting had a total diameter of 153 mm leaving a 23.5 mm air gap between the refractory surface and the oven wall. Figure 18 presents the casting process.

Figure 18. *The casting of the test tubes.*

The casted cement had to be left for drying for two to five days depending on the amount of water the masses had.

4.3 Development of the test procedure to obtain repeatable results

Before the samples can be tested they have to be dried. The first drying of the samples is done without the flow of water inside the metal pipes by heating the samples in the oven to a temperature of 110 °C to get the extra water to evaporate out from the ceramic material. This drying doesn't remove the crystallization water, which is removed later alongside the actual test runs. After spending at least 8 hours in the 110 °C oven, the oven can be switched off and the lid of the oven can be opened to let the possible moisture exit from the oven with natural flow of air.

In the beginning of the test runs, the system's hoses and the test pipes have to be filled with water from the water pipes of Tampere University of Technology (TUT) and the water has to be circulated in the test system's pipes and hoses until all of the air has come out from them. This can be monitored from the see-through outlet hose where the water is lead to the sewers of TUT. When no air bubbles are to be seen anymore, the water inlet valve is left open while shutting down the outlet valve, which causes a rise in the water pressure of the system. When the pressure level 0.8 bar for system start-up is reached, the inlet valve is also closed. If the water pressure is stable the water pump can be started. After the pump is started the pressure can be increased to the wanted level of about 1.5 bar by adding more water into the system. The velocity of the water can be altered with a valve to reach the wanted volume flow of 15 liters per minute.

When the water pump has been started, the oven can also be switched on. The guideline rate for the heating of the samples is 50 °C/h [19] to prevent the formation of cracks in the sample. When the oven reaches a temperature of about 650 °C the temperature is held in its place for several hours to remove the crystallization water from the samples. The crystallization water extraction happens approximately in the temperature of 540 °C [19]. After sustaining the temperature for several hours, the temperature of the oven is raised again at the velocity of 50 °C/h until the steel plates of the oven reach 850 °C which is the wanted test temperature. The samples are then left to warm up and become steady. The figure 19 shows the heating up process with the crystallization water removal period.

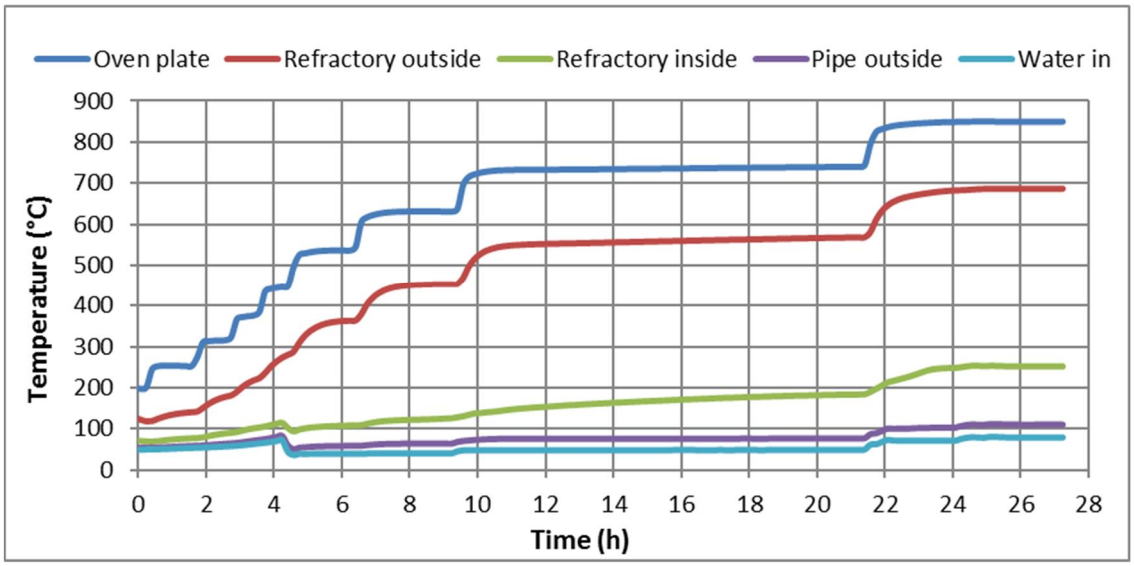

Figure 19. *Temperature curves during the heating up of the system.*

After the oven has reached the wanted temperature and the system's temperatures have settled, the temperature of the flowing water is set to about 80 °C with the help of a valve placed at the heat exchanger, which gets its cooling water from the cooling system of TUT. When the system has reached a steady state, meaning the temperatures haven't changed notably for few hours, the final test data can be gathered. The figures 20 and 21 show the changes in the test samples before and after the tests when the drying and removal of the crystallization water has occurred in the between.

Figure 20. *An LC-mass test sample before the tests.*

Figure 21. *An LC-mass test sample after the tests.*

The temperature data of the test samples, oven and water as well as the circulation flow data of the water are gathered into a computer via a data logger device for the analyzing of the test results. After the data gathering the oven's temperature can be lowered gradually at the rate of about 200 °C/h. When the test samples have reached a temperature lower than 100 °C, the power of the oven and the pumps can be shut down, since there is no more threat for the circulating water to begin boiling. Finally, when the samples have cooled down to room temperature, the systems pressure can also be released, which brings the system back to its starting point and the test run is completed.

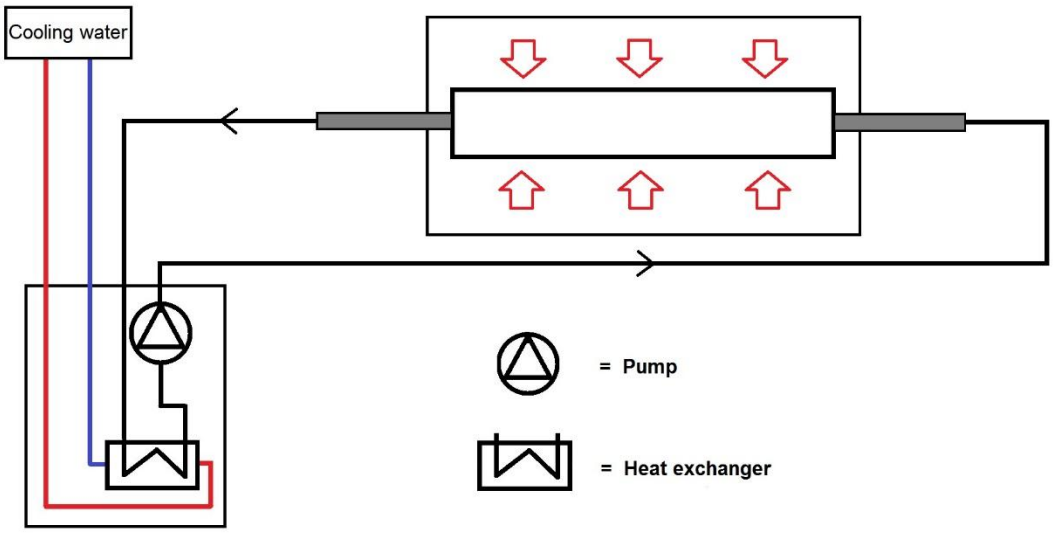

Figure 22. *A simplified figure of the process. Water is pumped into the system where it heats up inside the oven and then it is cooled down with the help of a heat exchanger.*

When running tests for the same sample more than once, the following test runs have the same procedures as the first one, with the exception that no drying or extraction of the crystallization water is needed. This means that the sample can be raised to the final temperature of the oven, 850 °C, without any pauses and the heating up can be done with a higher rate of 100 °C/h. Figure 22 shows the process when the tests are running.

4.4 Evaluation principles of the test results

The test results were analyzed using Microsoft Excel calculation sheets to determine the temperatures in various points of interest, the heat flow through the system, the thermal conductivity of the refractory material and the interfacial conductance between the steel pipe and the refractory. Even though the data series can consist of up to 10 000 measurements per signal, only the average value of the most stable part of about 200 to 300 measurement points were used in the evaluation of the results. Some of the measurement points have duplicate measurements and in these cases their average value is used in the calculations. Most of the temperatures were obtained as measurement data and the rest of the temperatures were calculated using the equations shown in the chapter 2. The heat flow, thermal conductivity and interfacial conductance were also calculated with the help of the presented theory of heat transfer.

The results were calculated using the electric circuit analogy where the flowing water inside the steel pipe was used as one of the ends of the circuit and the steel plates at the walls of the oven as the other end. The inlet and the outlet water temperatures were measured and they were used to find out the amount of heat transfer in the system. The average water temperature and the theory of convection were used to calculate the inner surface temperature of the steel pipe, which was also done by coming from the other side of the pipe by using the measured outer surface temperature of the pipe and the known thermal conductivity of the steel pipe.

The thermal conductivity of the refractory material was calculated with the help of two temperature measurements inside the refractory: one close to the inner surface and the other close to the outer surface. The thermal conductivity and the inner temperature measurement of the refractory were used to calculate the temperature at the inner surface of the refractory, which was then used with the steel pipe's outer surface temperature to receive the interfacial conductance between the pipe and the refractory. The outer surface temperature of the refractory was calculated with the knowledge of the thermal conductance and the measured temperature near the refractory's outer surface. This was also done with calculations using the temperature of the oven's steel plate and the theory of radiation and convection.

5. TEST RESULTS

The measurements were done at the premises of the Department of Material Sciences of TUT during a time period from January to June 2016. The results of the tests are presented in this chapter. Some of them are results of measurements and some of them are calculated with the help of the measured data.

5.1 Case 1: Bare tube

The first case is a bare steel tube without the refractory layer. The tests were done to see how the system works without having too many variables. Between the tests 1, 2 and 3 the water average temperatures were held at 63 °C, which was the maximum water temperature that was able to be reached in the test 1 where the oven's temperature was only 400 °C. As the water temperature was held constant, the oven's temperature was raised to 500 °C and 600 °C for the tests 2 and 3 respectively. The measured test results are presented in the tables 5 and 6.

Table 5. *The measured temperatures in the case 1.*

Measurement point	Test 1	Test 2	Test 3
	Temperature T [°C]	Temperature T [°C]	Temperature T [°C]
Water: in	62.7	62.6	62.5
Water: out	63.3	63.3	63.5
Pipe: outside surface 1	71.7	75.9	82.4
Pipe: outside surface 3	81.5	90.8	103.7
Pipe: outside surface 2	87.0	97.7	112.5
Oven	399.6	494.8	592.8

Table 6. *The measured volume flows in the case 1.*

	Test 1	Test 2	Test 3
Volume flow of water, $\dot{V}$ [l/min]	15.01	15.00	15.01

There were 3 thermocouple attachments on the steel pipe at the same distance longitudinally, but the temperature differences are caused by the angularly different placement, where the thermocouple 1 was placed on the side of the tube, the thermocouple 3 on the top of the tube and the thermocouple 2 was placed 45 degrees away from the other two measurement points at their middle point. This reveals the fact that even though there are

half a circle steel plates on the top and bottom of the oven, their effect on the flattening of the temperature distribution from the two electrical resistors is not perfect. The test tube was also turned angularly to make sure the effect wasn't due to thermocouple errors and the temperatures changed according to their position confirming the results. The calculated temperature distributions are presented in the table 7 and figure 23.

Table 7. *The temperatures at different radii of the system.*

		Test 1	Test 2	Test 3
	Radius *r* [mm]	Temperature *T* [°C]	Temperature *T* [°C]	Temperature *T* [°C]
Water	0.0	63.0	63.0	63.0
Pipe: inside surface	14.0	86.1	96.5	110.6
Pipe: outside surface	19.0	87.0	97.7	112.5
Oven wall	100.0	400.7	500.2	600.9

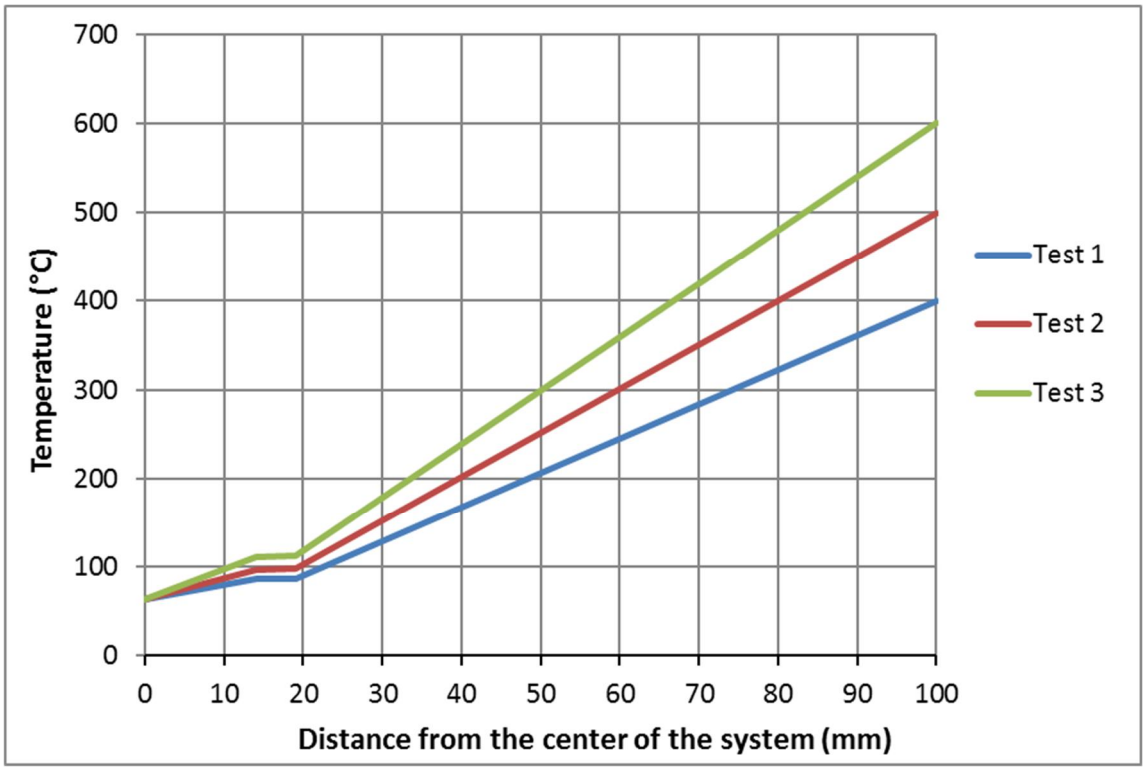

Figure 23. *Temperatures from the center of the pipe to the oven wall.*

The heat flow through the system into the water was calculated and the results are presented in the table 8 with the measured power of the oven and the calculated losses. The power of the oven was measured as a continuing current signal which average value during a test series was multiplied with the voltage that the oven uses.

Table 8. *The test results for case 2.*

	Test 1	Test 2	Test 3
Power of the oven, P_{tot} [W]	940.8	1415.0	2166.6
Heat flow through the system, Q_{sys} [W]	562.7	765.5	1086.5
Losses to surrounding room, Q_{loss} [W]	378.1	649.5	1080.2
Losses to surrounding room [%]	40.19	45.90	49.85

The results of the case 1 show that the testing rig is working well and that the thermocouple attachments should be placed at the same points angularly in all of the cases especially if the thermocouples are close to the surface of the test piece receiving the thermal radiation.

5.2 Case 2: Tube with conventional LC-cast layer without studs

The test tube in the case 2 is a steel tube with conventional LC-cast layer, which doesn't have studs to make the results more easily interpreted. The lack of studs, however, does cause some fear of the refractory layer to crack and fall off from the pipe surface due to different thermal expansion rates for steel and cement. This is why the drying of the cement without cooling water cycle was done at low temperatures of about 110 °C and the removal of crystallization water was done with the cooling water cycle to keep temperature rise of the steel pipe moderate to prevent major thermal expansion. The measured test results for case 2 are presented in the tables 9 and 10.

Table 9. *The measured temperatures in the case 2.*

	Test 1	Test 2	Test 3	Test 4	Test 5
Measurement point	T [°C]	T [°C]	T [°C]	T [°C]	T [°C]
Water: in	79.2	80.4	89.8	62.2	79.4
Water: out	80.9	81.9	91.4	63.7	81.2
Pipe: outside surface, 1	109.5	-	-	-	-
Pipe: outside surface, 2	107.1	108.9	117.1	93.4	111.7
Refractory: 5 mm, 1	255.2	281.1	286.1	272.8	289.4
Refractory: 5 mm, 2	250.1	263.7	268.8	254.8	270.8
Refractory: 45 mm, 1	690.9	696.4	698.4	693.4	701.8
Refractory: 45 mm, 2	699.6	703.1	705.0	700.2	711.9
Oven	843.8	843.5	844.2	842.6	846.3
Oven wall	850.9	849.2	849.9	848.2	-

Table 10. *The measured volume flows in the case 2.*

	Test 1	Test 2	Test 3	Test 4	Test 5
Volume flow of water, $\dot{V}$ [l/min]	15.01	15.09	15.07	15.16	15.03

Using the measured results, different temperatures for wanted sections of the system were calculated with help of the theory presented earlier in this work. The heat flow through the system, the interfacial conductance between the steel pipe and the refractory and the conductance of the refractory material were also calculated. The results are shown in the tables 11 and 12.

Table 11. *The temperatures at different radii of the system.*

		Test 1	Test 2	Test 3	Test 4	Test 5
	r [mm]	T [°C]	T [°C]	T [°C]	T [°C]	T [°C]
Water	0.0	80.1	81.1	90.6	62.9	80.3
Pipe: inside surface	14.0	105.4	106.1	114.4	90.8	108.6
Pipe: outside surface	19.0	108.3	108.8	117.0	93.3	111.7
Refractory: surface in	19.0	147.2	170.6	176.4	160.7	178.4
Refractory: 5 mm	24.0	252.6	272.4	277.4	263.8	280.1
Refractory: 25 mm	44.0	526.2	536.5	539.6	531.4	543.8
Refractory: 45 mm	64.0	695.2	699.8	701.7	696.8	706.9
Refractory: surface out	74.0	760.8	763.1	764.5	761.0	770.1
Oven wall	100.0	850.9	849.2	849.9	848.2	850.3

Table 12. *The test results for case 2.*

	Heat flow Q [W]	Interfacial conductance h_i [W/m^{2}K]	Conductivity at 550 °C k_r [W/mK]	U-value $U_{A,out}$ [W/m^{2}K]
Test 1	1704.7	610.0	1.00	5.58
Test 2	1610.4	363.6	0.98	5.26
Test 3	1613.5	379.7	0.99	5.33
Test 4	1586.6	328.9	0.95	5.08
Test 5	1851.1	387.4	1.13	6.02

The table 11 presents the temperatures at different measurement points and surfaces and the table 12 shows the calculated results for interfacial conductance between the steel tube and the refractory, the thermal conductivity of the refractory and the U-value for the cylindrical system calculated with the outside surface area of the refractory with the radius r_3 as presented in the figure 1 with the other factors. Tests 3 and 4 were done at different water temperatures in case later test for different refractory materials turn out impossible to run at the original 80 °C. The first test was done separately from the later ones, which means the oven's temperature was brought down between tests 1 and 2. This might have caused a small gap between the pipe and the refractory due to different thermal expansion rates of the two different materials, which can be seen as a larger temperature difference at the interface. The tests 2, 3 and 4 were done during the same test run, and between the tests, only the water temperature was changed by adjusting the level of the heat exchanger

of the water cycle. The test 5 was done several weeks later to see if the interface had changed even more after the previous tests. The results show that it had not since the interfacial conductance had stayed constant. The gap between the steel pipe and the refractory was measured after the test 5 with a feeler gauge and the width of the gap was approximately 50 µm at most at one section of the pipe where the feeler gauge was possible to be slid into the interface. The results for the tests 2, 3 and 4 are clear as the temperature changes are following the change of water temperature. The results are also presented in the figures 24, 25 and 26.

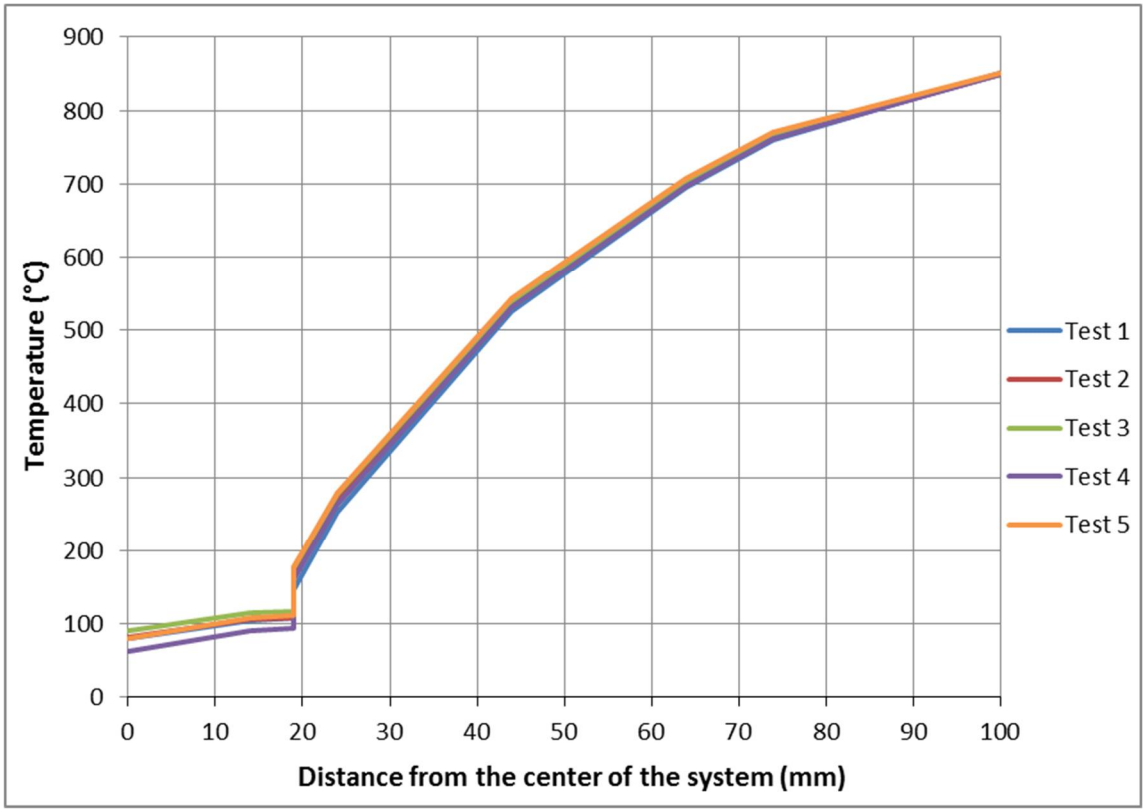

Figure 24. *Temperatures from the center of the pipe to the oven wall.*

The temperature profile shows clearly that heat is transferred at the same rate through the refractory in all of the cases. The differences in the interface are clearer in the following figure 25 where the system is zoomed in.

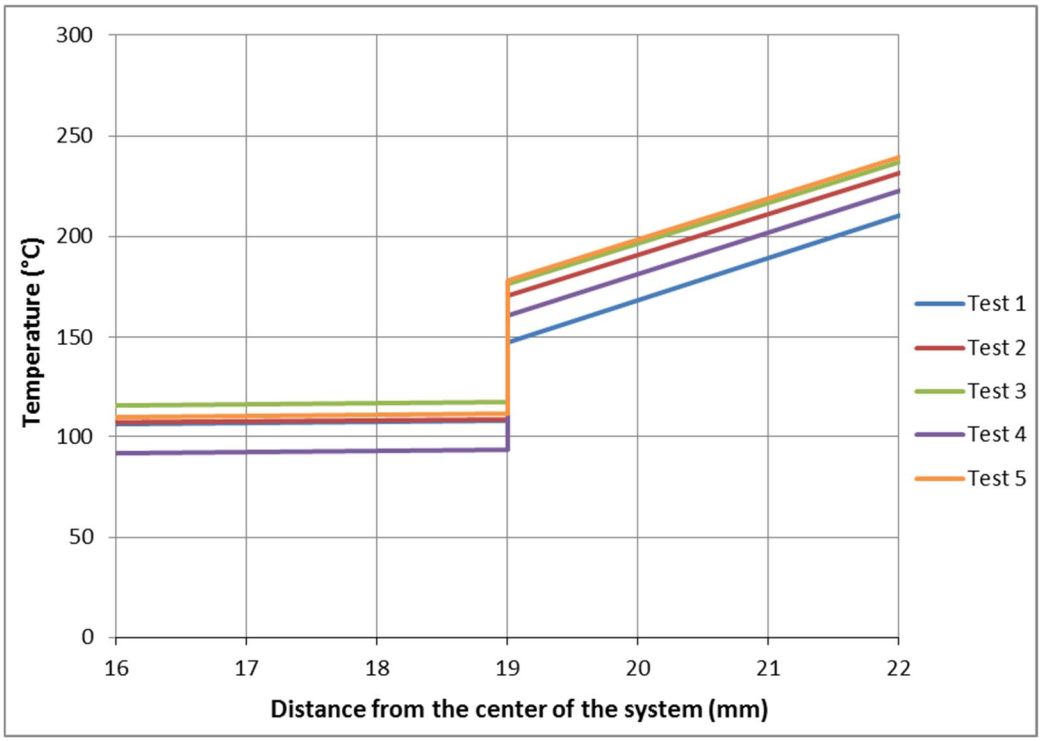

Figure 25. *Temperatures at the interface.*

The figure 25 shows that the temperature rises in the interface during the test 1 is significantly lower than during the other tests. This is even easier to see in the figure 26, where the tests 3 and 4 are taken out of the picture, as these tests were ran at different water temperatures than the 80 °C in the tests 1, 2 and 5.

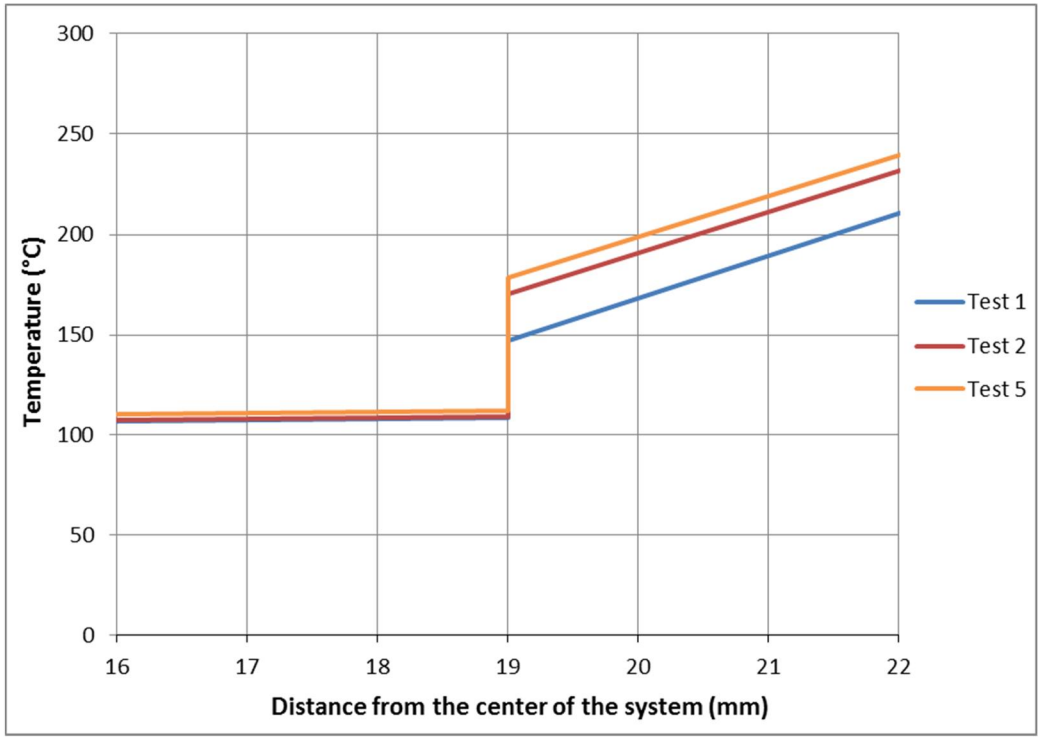

Figure 26. *Temperatures at the interface when water temperature is 80 °C.*

The test results for LC-casted refractory were clear as the measured thermal conductivities were in all of the test runs either 1.0 W/mK or 1.1 W/mK. This result is surprisingly close to the value given by the material provider whose estimate for thermal conductivity of the material was 1.1 W/mK.

5.3 Case 3: Tube with conventional LC-cast layer with studs

The test tube in the case 3 is a steel tube with conventional LC-cast layer, that has studs keeping the refractory at the steel tube as in the real power plants. The studs prevent the refractory from falling off from the tubes if minor cracks are formed. The pre-drying of the cement without cooling water cycle was done at low temperatures of about 110 °C and the removal of crystallization water was done with the cooling water cycle to keep temperature rise of the steel pipe moderate to prevent major thermal expansion. The measured test results for case 3 are presented in the tables 13 and 14.

Table 13. *The measured temperatures in the case 3.*

Measurement point	Test 1	Test 2	Test 3	Test 4
	Temperature T [°C]	Temperature T [°C]	Temperature T [°C]	Temperature T [°C]
Water: in	80.0	80.5	89.8	61.9
Water: out	82.4	82.8	92.1	64.3
Refractory: 5 mm, 1	282.0	283.3	289.8	272.8
Refractory: 5 mm, 2	272.0	272.7	279.2	262.1
Refractory: 45 mm, 1	655.7	655.9	659.5	651.0
Refractory: 45 mm, 2	653.1	653.0	656.0	648.6
Stud: 3 mm	235.9	236.6	243.2	224.9
Stud: 47 mm	575.8	575.3	578.1	570.4
Oven	840.6	840.6	841.6	839.3

Table 14. *The measured volume flows in the case 3.*

	Test 1	Test 2	Test 3	Test 4
Volume flow of water, $\dot{V}$ [l/min]	14.97	15.06	15.00	14.36

Using the measured results, different temperatures for wanted sections of the system were calculated. The heat flow through the system, the interfacial conductance between the steel pipe and the refractory and the conductance of the refractory material were also calculated. The results are shown in the tables 15 and 16.

Table 15. *The temperatures at different radii of the system.*

		Test 1	Test 2	Test 3	Test 4
	r [mm]	Temperature T [°C]	Temperature T [°C]	Temperature T [°C]	Temperature T [°C]
Water	0.0	81.2	81.6	90.9	63.1
Pipe: inside surface	14.0	114.9	115.3	109.9	99.4
Pipe: outside surface	19.0	119.0	119.2	121.5	103.2
Refractory inside surface	19.0	187.1	188.4	195.6	176.4
Refractory: 5 mm	24.0	277.0	278.0	284.5	267.5
Refractory: 25 mm	44.0	510.2	510.6	515.2	503.7
Refractory: 45 mm	64.0	654.4	654.4	657.7	649.8
Refractory outside surface	74.0	710.3	710.2	713.0	706.4
Stud: 3 mm	22.0	235.9	236.6	243.2	224.9
Stud: 47 mm	66.0	575.8	575.3	578.1	570.4
Oven wall	100.0	848.6	848.6	849.6	847.3

Table 16. *The test results for case 3.*

	Heat flow Q [W]	Interfacial conductance h_i [W/m^{2}K]	Conductivity at 550 °C k_r [W/mK]	U-value $U_{A,out}$ [W/m^{2}K]
Test 1	2474.8	508.2	1.71	8.94
Test 2	2307.7	466.2	1.60	8.34
Test 3	2314.6	470.1	1.61	8.44
Test 4	2316.4	442.7	1.58	8.21

The table 15 presents the temperatures at different measurement points and surfaces and the table 16 shows the calculated results for interfacial conductance between the steel tube and the refractory, the thermal conductivity of the refractory and the U-value for the cylindrical system calculated with the outside surface area of the refractory with the radius r_3 as presented in the figure 1 with the other factors. Tests 3 and 4 were done at different water temperatures in case later test for different refractory materials turn out impossible to run at the original 80 °C. The first test was done separately from the later ones, which means the oven's temperature was brought down between the tests 1 and 2. Unlike in the previous case without anchoring of the refractory, the gap formed between the tests 1 and 2 is a lot smaller due to the fact that the steel studs were holding the refractory on its place regardless of the different thermal expansion rates of the steel pipe and the refractory. The tests 2, 3 and 4 were done during the same test run, and between the tests, only the water temperature was changed by adjusting the level of the heat exchanger of the water cycle. The results for the tests 2, 3 and 4 are clear as the temperature changes are following the change of water temperature. The temperature results are also presented in the figures 27 and 28.

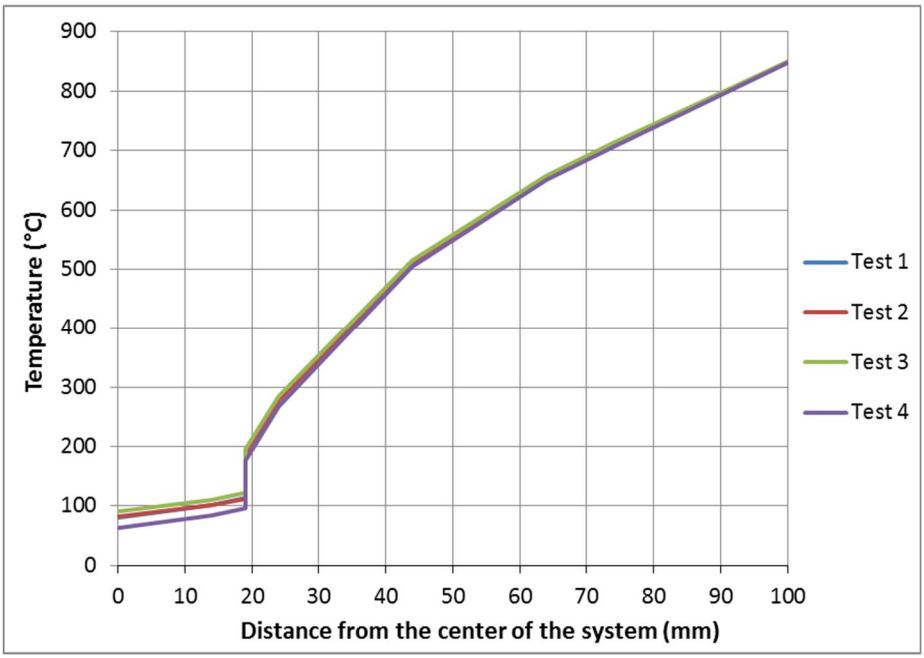

Figure 27. *Temperatures from the center of the pipe to the oven wall*

The results for the tests 2, 3 and 4 are clear as the temperature changes are following the change of water temperature and for tests 1 and 2 they are almost identical. The temperature behavior at the interface can be seen more clearly in the following figure 28.

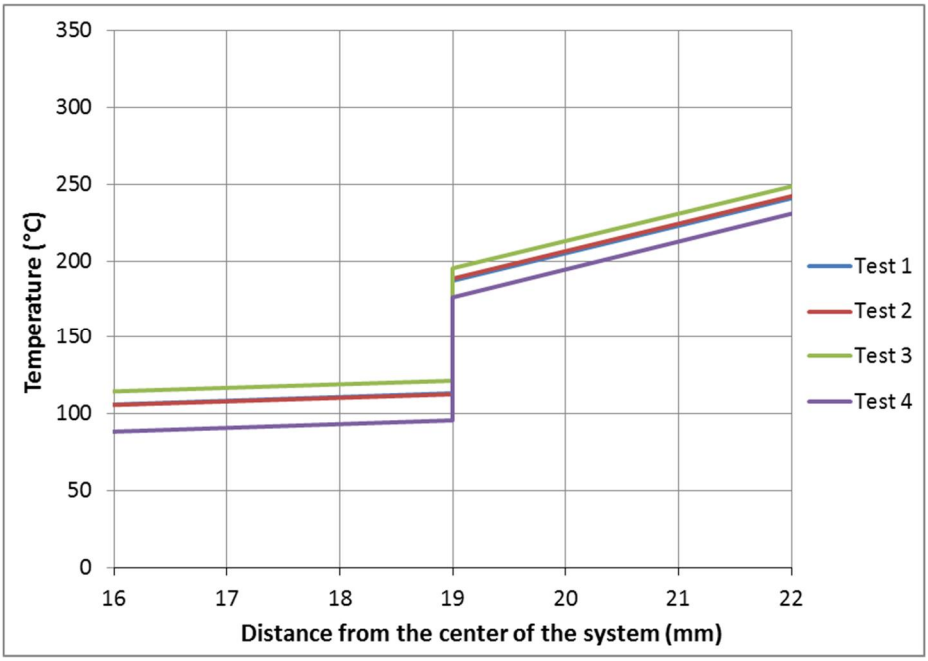

Figure 28. *Temperatures at the interface.*

The results show that the steel studs increased the overall conductivity inside the refractory to 1.6 – 1.7 W/mK from the 1.0 – 1.1 W/mK in the studless case. This can also be seen in the amount of heat flow which increases from 1600 W to 2300 W when the studs are added to the system.

5.4 Case 4: Tube with insulating cast layer without studs

The test tube in the case 4 is a steel tube with conventional insulating cast layer, which doesn't have studs to make the results more easily interpreted. Similarly to the case 2, the lack of studs causes some fear of the refractory layer to crack and fall off from the pipe's surface due to different thermal expansion rates for steel and cement. This is why the drying of the cement without cooling water cycle was done at low temperatures of about 110 °C and the removal of crystallization water was done with the cooling water cycle to keep temperature rise of the steel pipe moderate to prevent major thermal expansion. The measured test results for case 4 are presented in the tables 17 and 18.

Table 17. *The measured temperatures in the case 4.*

Measurement point	Test 1	Test 2
	Temperature T [°C]	Temperature T [°C]
Water: in	62.6	61.5
Water: out	63.1	62.0
Pipe: outside surface	78.4	80.2
Refractory: 5 mm	280.1	285.0
Refractory: 25 mm	556.8	560.3
Refractory: 45 mm	724.2	726.7
Oven	853.5	854.3

Table 18. *The measured volume flows in the case 4.*

	Test 1	Test 2
Volume flow of water, $\dot{V}$ [l/min]	15.01	15.0

Using the measured results, different temperatures for wanted sections of the system were calculated. The heat flow through the system, the interfacial conductance between the steel pipe and the refractory and the conductance of the refractory material were also calculated. The results are shown in the tables 19 and 20.

Table 19. *The temperatures at different radii of the system.*

		Test 1	Test 2
	Radius r [mm]	Temperature T [°C]	Temperature T [°C]
Water	0.0	62.8	61.8
Pipe: inside surface	14.0	77.6	79.3
Pipe: outside surface	19.0	78.3	80.1
Refractory: inside surface	19.0	173.5	178.9
Refractory: 5 mm	24.0	280.1	285.0
Refractory: 25 mm	44.0	556.8	560.3
Refractory: 45 mm	64.0	724.2	726.7
Refractory: outside surface	74.0	789.1	791.2
Oven wall	100.0	850.5	851.3

Table 20. *The test results for case 4.*

	Heat flow Q [W]	Interfacial conductance h_i [W/m^{2}K]	Conductivity at 450 °C $k_{r,in}$ [W/mK]	Conductivity at 650 °C $k_{r,out}$ [W/mK]	U-value $U_{A,out}$ [W/m^{2}K]
Test 1	502.7	73.8	0.292	0.299	1.52
Test 2	514.2	72.7	0.300	0.307	1.55

The table 19 presents the temperatures at different measurement points and surfaces and the table 20 shows the calculated results for interfacial conductance between the steel tube and the refractory, the thermal conductivity of the refractory and the U-value for the cylindrical system calculated with the outside surface area of the refractory with the radius r_3 as presented in the figure 1 with the other factors. Tests 1 and 2 were done separately from each other. Because the mass of the refractory material in the case 4 was highly insulating, the tests turned out to be impossible to run at the planned 80 °C, which is why the temperature of about 60 °C was chosen as the goal temperature as in the test 4 of case 2. The thermal conductivity of the system was able to be calculated separately from the inner and outer part of the refractory as one additional temperature measurement point was added to the middle of the refractory when in the cases 2 and 3 the thermocouple attachments inside the refractory were installed only to the proximity of the inner and outer surfaces. The interfacial conductance in these tests are really low, which is probably due to the high porosity of the mass leaving only a small contact are between the pipe and the refractory. The temperature results are also presented in the figure 29.

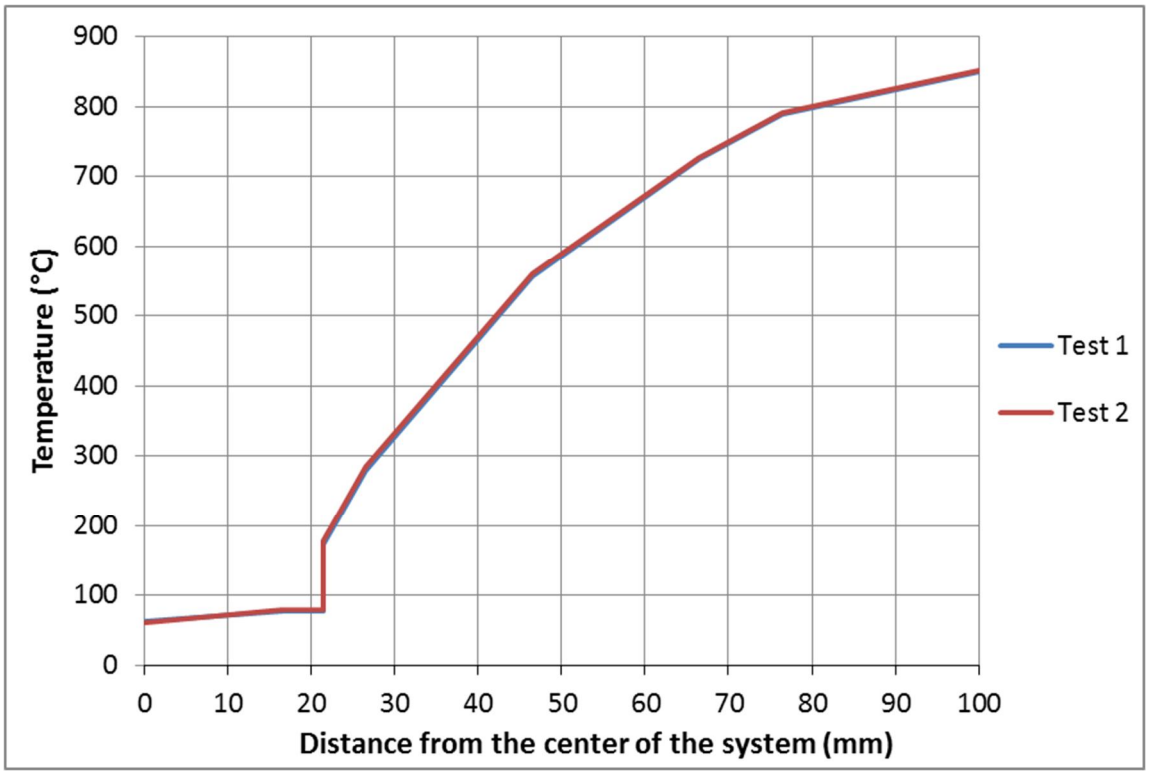

Figure 29. *Temperatures from the center of the pipe to the oven wall*

The results for both of the tests were identical as can be seen very clearly in the figure 28. The overall conductivity inside the refractory was about 0.30 W/mK, which is slightly different from the value estimation of 0.2 W/mK by the material provider, but they are still at the same order of magnitude. It is also apparent that the conductivity of the material increases a bit with higher temperatures as can be seen in the table 20.

5.5 Case 5: Tube with medium conductivity SiC-cast layer without studs

The test tube in the case 5 is a steel tube with medium performance SiC-cast layer, which doesn't have studs to make the results more easily interpreted. As mentioned in the earlier cases, this causes some fear of the refractory layer to crack and fall off from the pipe surface due to different thermal expansion rates for steel and cement. This is why the drying of the cement without cooling water cycle was done at low temperatures of about 110 °C and the removal of crystallization water was done with the cooling water cycle to keep temperature rise of the steel pipe moderate to prevent major thermal expansion. The measured test results for case 2 are presented in the tables 21 and 22.

Table 21. *The measured temperatures in the case 5.*

Measurement point	Test 1	Test 2	Test 3
	Temperature T [°C]	Temperature T [°C]	Temperature T [°C]
Water: in	75.9	73.6	61.5
Water: out	80.0	77.7	65.4
Pipe: outside surface	124.5	123.9	104.8
Refractory: 5 mm	209.3	215.5	209.8
Refractory: 25 mm	353.7	365.9	362.5
Refractory: 45 mm	463.0	476.3	473.5
Oven	731.9	736.4	734.2

Table 22. *The measured volume flows in the case 5.*

	Test 1	Test 2	Test 3
Volume flow of water, $\dot{V}$ [l/min]	14.87	15.02	15.01

Using the measured results, different temperatures for wanted sections of the system were calculated. The heat flow through the system, the interfacial conductance between the steel pipe and the refractory and the conductance of the refractory material were also calculated. The results are shown in the tables 23 and 24.

Table 23. *The temperatures at different radii of the system.*

		Test 1	Test 2	Test 3
	Radius r [mm]	Temperature T [°C]	Temperature T [°C]	Temperature T [°C]
Water	0.0	77.9	75.6	63.5
Pipe: inside surface	14.0	117.3	116.9	98.0
Pipe: outside surface	19.0	124.5	123.9	104.8
Refractory: inside surface	19.0	153.6	157.6	150.9
Refractory: 5 mm	24.0	209.3	215.5	209.8
Refractory: 25 mm	44.0	353.7	365.9	362.5
Refractory: 45 mm	64.0	463.0	476.3	473.5
Refractory: outside surface	74.0	505.4	519.1	516.6
Oven wall	100.0	751.9	756.4	754.2

Table 24. *The test results for case 5.*

	Heat flow Q [W]	Interfacial conductance h_i [W/m^{2}K]	Conductivity at 300 °C $k_{r,in}$ [W/mK]	Conductivity at 450 °C $k_{r,out}$ [W/mK]	U-Value $U_{A,out}$ [W/m^{2}K]
Test 1	4173.4	2004.0	4.64	3.80	23.1
Test 2	4085.4	1695.2	4.37	3.68	21.8
Test 3	3986.9	1207.4	4.20	3.57	20.5

The table 23 presents the temperatures at different measurement points and surfaces and the table 24 shows the calculated results for interfacial conductance between the steel tube and the refractory, the thermal conductivity of the refractory and the U-value for the cylindrical system calculated with the outside surface area of the refractory with the radius r_3 as presented in the figure 1 with the other factors. Test 1 was done separately from the tests 2 and 3 and between the tests 2 and 3 only the water temperature was adjusted. Because the mass of the refractory material in the case 5 was a conducting mass, the heat flowed through the system at such a high rate, that it was impossible to raise oven's temperature to the 850 °C, thus the maximum temperature of 750 °C was used. During to tests there were also some problems with the cooling water cycle due to water temperature changes in the cooling water pipes, which meant that stable test conditions were difficult to reach. This combined with the enormous amount of heat flow through the system made the water temperatures almost impossible to adjust, which can be seen in the water temperatures of the tests 1 and 2 where the target temperature was 80 °C. This of course doesn't have any impact on the conductivity of the refractory but it effects on the temperature curves. The overall conductivity inside the refractory was measured from two different radii, as there where three temperature measurement points inside the refractory as in the case 4. The temperature results are also presented in the figure 30.

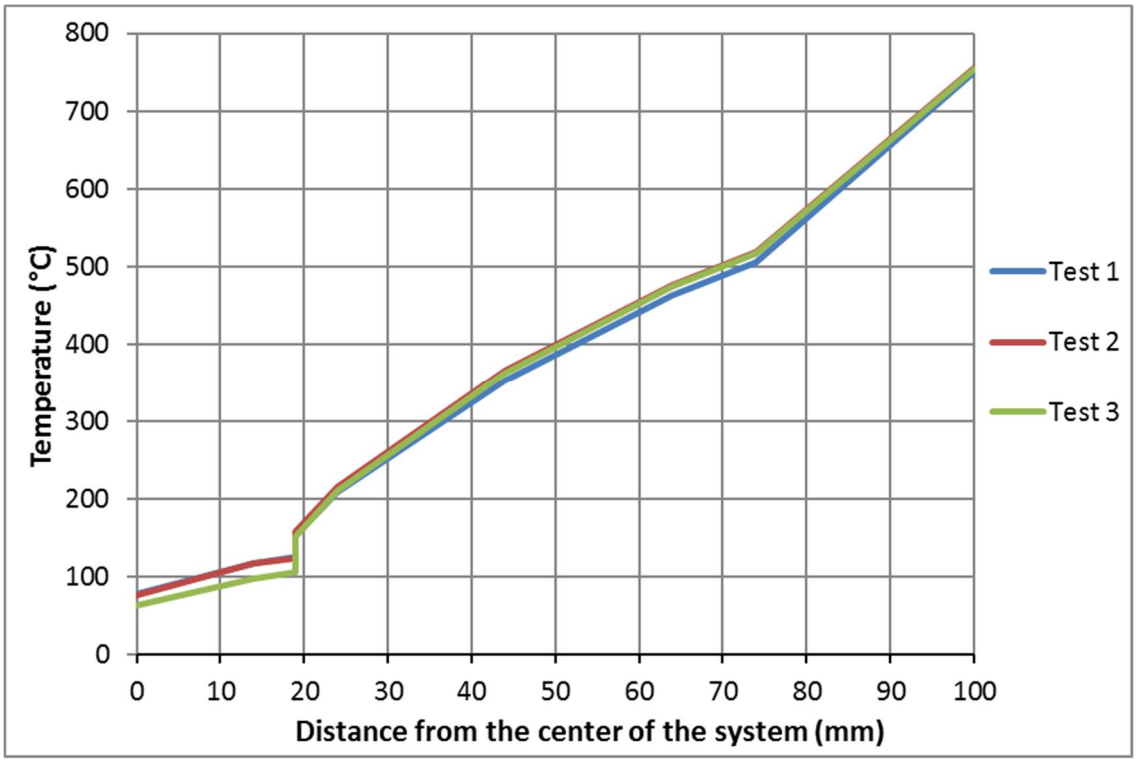

Figure 30. *Temperatures from the center of the pipe to the oven wall.*

The test 1 had slightly lower temperature increase through the refractory, which is at the distance of 19 – 74 mm from the center of the system. This can be seen as the higher thermal conductance result in the table 24. The odd result in this case was the temperature behavior inside the interface as can bee seen in the following figure 31.

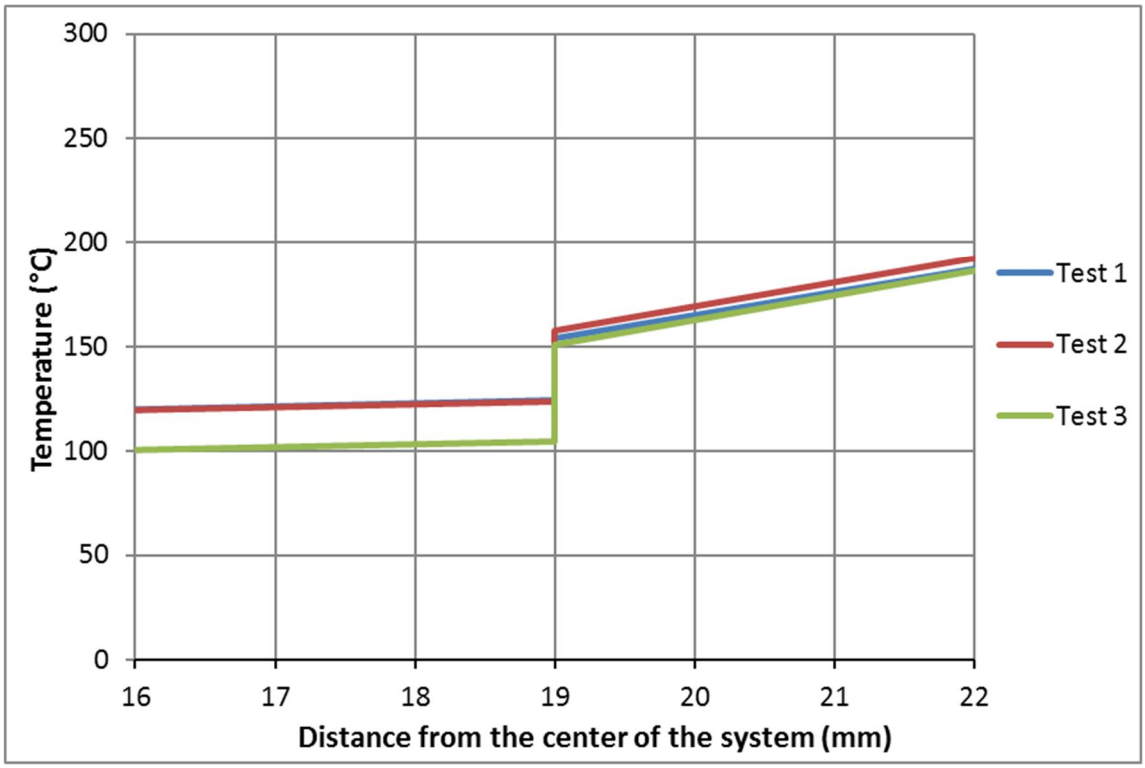

Figure 31. *Temperatures at the interface.*

The temperature difference between the steel pipe outer surface and the refractory inside surface is almost the double in the test 3 compared to the tests 1 and 2. The test 3 was ran with a lower water temperature, but because the amount of heat transfer was so huge, it didn't have a huge impact on the refractory temperature. the differences can also be seen in the interfacial conductivity values in the table 24. The values for thermal conductance in the refractory were measured from the inner and the outer parts of the refractory and there was a significant difference in their values. For the inner part that was at the temperature of aproximately 300 °C the thermal conductivity was 4.4 W/mK and for the outer part where the temperature was aproximately 400 °C the thermal conductivity got a value of 3.7 W/mK. The estimated value for thermal conductivity by the material provider was 5.8 W/mK, which is also a bit different from the measured results. These differences are probably caused by the relatively high conductivity of the material which makes it more unpredictable to estimate. The results also suggest that the thermal conductivity of this particular material rises when the the temperature rises.

5.6 Comparison of different masses

The cases in this study involved measurements with three different refractory masses. In the cases 2, 4 and 5 different masses: 1, 2 and 3 respectively, had been used and the test

tubes didn't have any studs interfering with the results. The thermal conductivities received with the tests are presented in the following table 25.

Table 25. *The thermal conductivities of different refractory masses*

	Conductivity at 300 °C k_r [W/mK]	Conductivity at 450 °C k_r [W/mK]	Conductivity at 550 °C k_r [W/mK]	Conductivity at 650 °C k_r [W/mK]
Case 2: Mass 1	-	-	1.0	-
Case 4: Mass 2	-	0.30	-	0.31
Case 5: Mass 3	4.4	3.7	-	-

As it makes sense, the conductivity of the insulating mass 2 is very low and the conductivity of the semi-conducting SiC mass 3 is the highest although not as high as it was expected. The conduction of the SiC mass also decreases notably when temperature rises, at least inside this temperature range. The temperatures mentioned in the table 25 are the mean temperatures between the refractories different measurement points. The radial temperature distribution inside the studied system is shown in the figure 32.

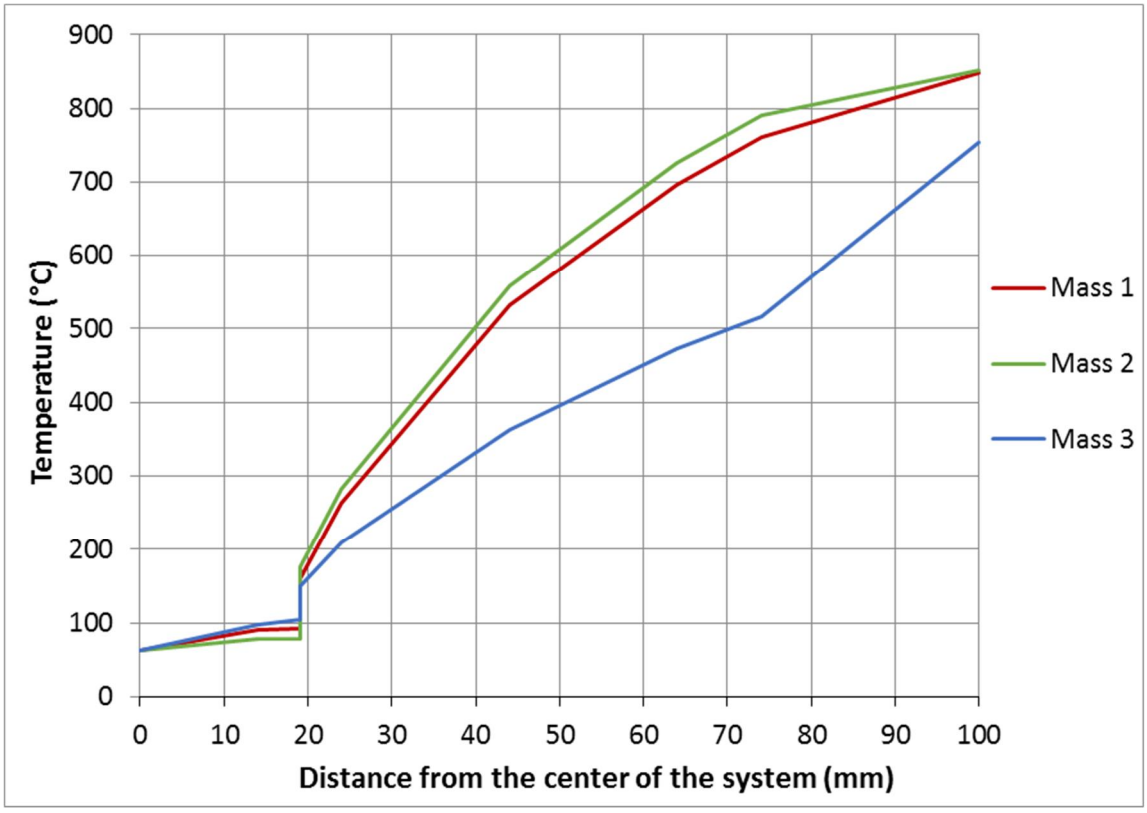

Figure 32. *The temperature distribution for the test tubes with different masses when the water temperature is 60 °C.*

The curve for mass 3 in the figure 32 should be slightly steeper, but the mass was such a conducting one that the oven couldn't reach the wanted 850 °C temperature due the high rate of heat transfer to the cooling water cycle. Nevertheless, it is clear that the mass 2

has the highest resistance for the heat transfer and the mass 3 has the highest heat conduction of the three studied masses. The interfacial conductance is presented more clearly in the figure 33.

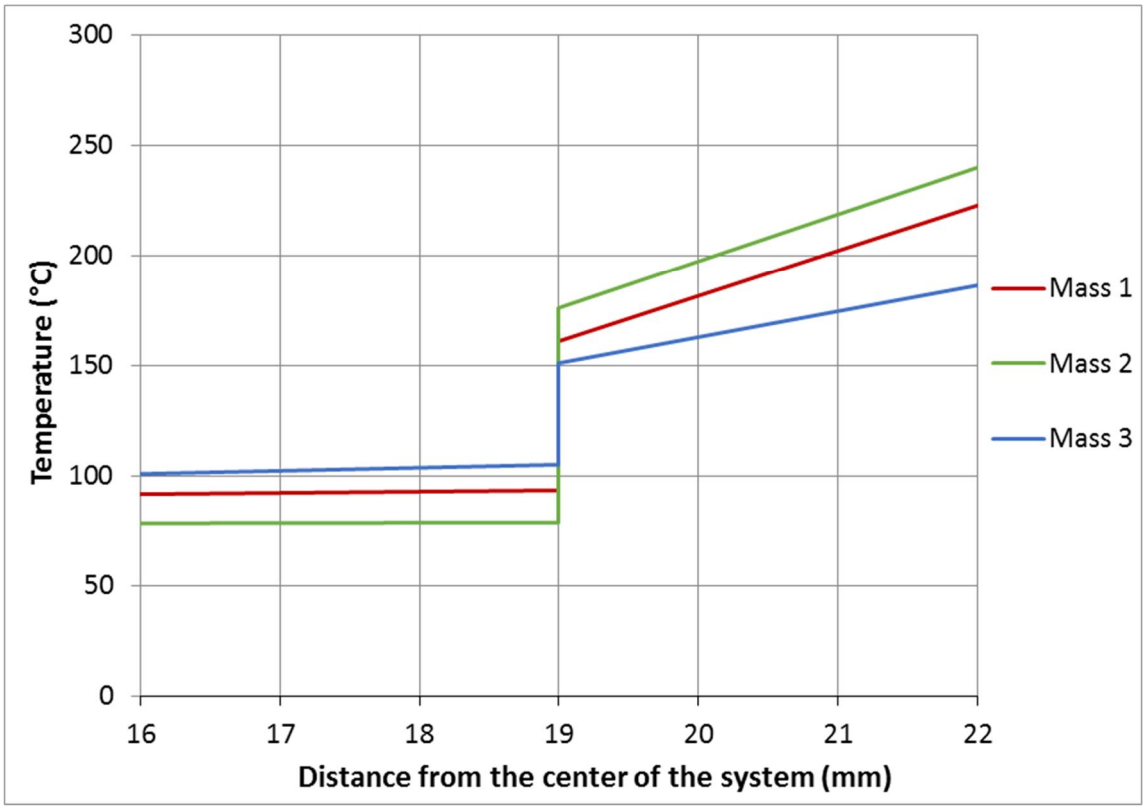

Figure 33. *The zoomed in temperature distribution near the interface for the test tubes with different masses when the water temperature is 60 °C.*

The great differences in the temperature profiles between the three masses in the figure 33 are explained largely with the fact that the amount of heat transfer through the refractory layer varied very much with the different masses. The average values for the heat flow in the different cases were approximately: 1600 W for the case of the first mass, 500 W for the case of the second mass and 4000 W for the case of the third mass. These differences, however, don't have influence on the values for the calculated thermal conductivities.

6. ERROR EVALUATION

Because the test rig was new and used the first time in this study there are some factors that might have caused errors to results. The most significant effect that has an impact on the thermal conductivity results comes from the heat flow calculations, which were done by using the properties of the water flow inside the steel pipe. The temperatures for the calculations were measured from both ends of the oven with thermocouple rods that were slid through the connectors that connected the water distribution hoses to the test tubes. Although the distance between the two thermocouples was known, their exact distance to the steel pipe's wall was not. The thermocouples were kept off from the walls with the help of a ring with three studs at 120 degree differences from each other, but because the entrance to the pipe was narrower than the pipe itself, it was impossible to construct the rings with long enough studs to keep the temperature measurements at the exact centerline of the pipe. This possible error is however lessened by the fact that the flow inside the pipe was turbulent leading to good mixing of the water and increasing the accuracy of the mean temperature measurements.

The turbulent water flow inside the pipe was not fully developed, which meant that the equations for determining the convective heat transfer coefficient from water to steel pipe are not totally accurate due to the unknown boundary surface thickness. This wasn't a huge problem since the temperatures at the pipe's outside surface were measured and the conductivity of the steel pipe was known.

The thermocouple measurements may have some error in their reading and for the K-type thermocouples used in this study the accuracy is ± 2.2 °C or ± 0.75 % depending on whichever is greater [20]. This means that for example for a reading of 600 °C the accuracy is ± 4.5 °C. Other error factor concerning the thermocouples is their placement. The effect of the angular placement is clear from the case 1 with the bare tube, where highest temperatures were reached from the point which was facing straight to the electric resistors of the oven and the lowest temperatures from the point that was facing the hinges in the middle of the two resistors on top and below of the oven. The effect was lessened by installing the half a circle metal plates, but the heat distribution wasn't still perfect. The angular placement has the biggest effect for points close to the surface because the temperatures are smoothing up when going inwards from the surface of the refractory. This effect was taken care by not placing the thermocouple that was closest to the surface right on the top or the side of the tube and also by placing the thermocouples to same spots in all of the test runs.

The third possible error factor concerning the thermocouples is that the attachment of the thermocouple rods was done by bending them to the correct distances. This method is

good and works well for its purpose, but the casting of the refractory has to be done carefully and calmly in order to prevent touching the thermocouples because that might result to undesirable bend or other movement of a thermocouple. Even if the thermocouples are not touched, it is possible that slight bending might happen due to the sudden weight of the mass. This might lead to serious errors in the results if the temperature was measured at a different distance from the pipe surface as was thought.

The oven planned for this study had a heating power of 6000 W and it worked in a way that it was either on with full power or then it was off completely, which means that if for example during a test the oven was taking an average power of 1000 W, it meant that it was on every sixth second on average. During the tests of case 5, however, the oven was on all the time due to the high thermal conductivity of the mass, but the heat flow to the cooling water cycle was only about 4000 W, which raised questions on the correctness of the results. A thermal imaging camera was used to monitor the oven's outer surface temperatures and they revealed that the sides of the oven were not as well insulated as expected having outside temperatures of 120 – 280 °C when the inside temperature was 850 °C. This meant that the losses of 2000 W by radiation to the surrounding room were more than possible. The two ends of the oven were well insulated as their temperatures were left under 100 °C. An image taken with the thermal imaging camera is presented in the figure 34 below.

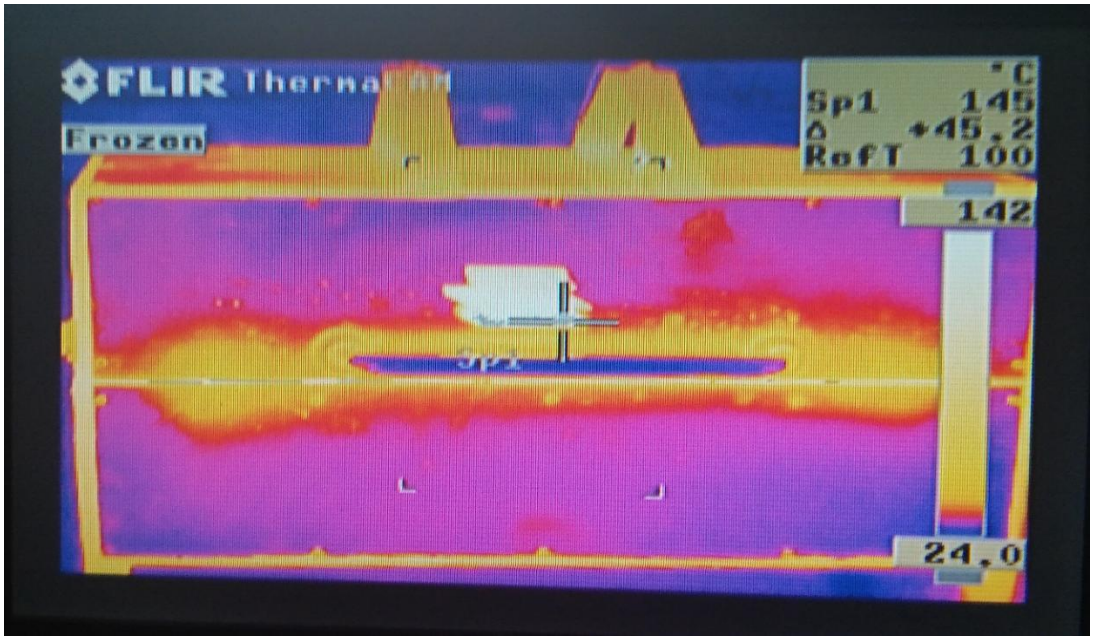

Figure 34. *An image taken with the thermal imaging camera from the front of the oven. The white measured area is a black matte surface tape.*

The image in the figure 33 shows the temperature distribution with the emissivity set to 1.0 for the black matte surface taping, which makes the other parts look a lot cooler in the image than in reality. When the temperatures of the taped area were found out, the emissivity was set to the correct level and the temperatures mentioned above were measured.

Final possible source for errors is the fact that even if the casting of the refractory is done perfectly, there still exists homogeneity and some of the grains might be big with a diameter of even 5 mm. This would cause misleading results due to higher or lower thermal conductivity through a specific route when compared to the average value. This factor is lessened in this study through to the big full scale sample size minimizing the effect of a single large grain, which might have a huge impact on the more conventional small scale thermal conductivity tests.

7. CONCLUSIONS

The purpose of this study was to develop a test procedure for testing a cylinder shaped multi-layer system consisting of a steel pipe and a refractory layer to find out the thermal conductivity of the refractory material. The test rig consisted of a cylindrical oven and a water distribution system with adjustable levels for water temperature, pressure and volume flow in the system. Three different refractory masses were tested and the results for temperature distributions inside the test pieces were gathered into a computer for the determination of the thermal conductivity. In addition to the thermal conductivity of the refractory mass the interfacial conductance between the steel pipe and the refractory was examined. After some adjustments and modifications of the equipment, the test procedures turned out to be well working and easily duplicated.

The test results presented in the chapter 5 showed that the conductivity estimates given by the material providers were close to the ones received with the tests. The exact value that should be used in the modelling of the actual heat transfer process in a power plant system is not still hundred percent sure but at least the fact that different test runs for a single material gave almost identical values for the conductivity makes the test results quite trustworthy. The effect of steel studs inside the refractory was also studied and a value for the total thermal conductivity through the studded refractory layer was given to compare it to the value obtained from earlier test runs without the studs.

The third objective in this study was to examine the interfacial conductance between the steel pipe and the refractory. As expected, minor gap formation happened at the interface without studs to keep the refractory at its place, but after the formation had happened, it stayed the same for the rest of the tests. This could be seen in the results as weakening conductance through the interface. The decrease in the value of the interfacial conductance didn't occur at such a high rate when the test tube was studded. The calculated values for interfacial conductance cannot be used as such because they vary a lot by many things that cannot be controlled during the installation such as contact pressure. But the phenomena of gap formation itself is an important thing to take into consideration during the planning process.

In conclusion, a test procedure for the testing of thermal conductivity of a refractory in a cylindrical system was planned and executed and the procedure worked as it was planned as trustworthy and repeatable test results were obtained. Thus, the equipment can be used also in the future to examine the heat transfer of different masses or other type of cylindrical multi-layer systems, which may contain steel anchors instead of the steel studs inside the refractory or some kind of thin coating on the steel pipe to reduce the interface's insulating effect on the heat transfer.

REFERENCES

[1] A. F. Mills, *Basic Heat & Mass Transfer*, Second edi. New Jersey, USA: Prentice Hall, Inc., 1999.

[2] S. P. Sukthame, *A Textbook On Heat Transfer*, Fourth edi. Hyderabad, India: Universities Press Ltd., 1971.

[3] NIST, "Reference on Constants, Units and Uncertainty." [Online]. Available: http://physics.nist.gov/cgi-bin/cuu/Value?sigma. [Accessed: 08-May-2016].

[4] A. Aziz, *Heat Conduction with Maple*, First edit. Spokane, USA: John Wiley & Sons Inc., 2007.

[5] MIT, "'Laplace's equation in cylindrical coordinates.'" [Online]. Available: http://web.mit.edu/6.013_book/www/chapter5/5.7.html. [Accessed: 01-Jul-2016].

[6] F. J. Bayley, J. M. Owen, and A. B. Turner, *Heat Transfer*, First edit. New York, USA: Barnes and Noble Book Co., 1972.

[7] C. J. Glassbrenner and G. A. Slack, "Thermal Conductivity of Silicon and Germanium from 3 °K to the Melting Point," *Phys. Rev. Lett.*, no. 134, 1964.

[8] P. G. Guest, *Numerical Methods of Curve Fitting*, First edit. Sydney, Australia: Cambridge University Press, 1961.

[9] Thermopedia, "Thermal Contact Resistance." [Online]. Available: http://www.thermopedia.com/content/1188/. [Accessed: 28-Jan-2016].

[10] M. G. Cooper and B. B. M. and M. M. Yovanovich, "Thermal Contact Conductance," *Int J. Heat Mass Transf.*, vol. 153, pp. 317–23, 1969.

[11] C. V Madhusudana, *Thermal Contact Conductance*, Second edi. Sydney: Springer, 2014.

[12] P. Teertstra, "Thermal Conductivity And Contact Resistance Measurements For Adhesives," Vancouver, Canada, 2007.

[13] Refractory Mass Provider, *Technical Data Sheet Of The Low Cement Refractory Mass*. 2015.

[14] Refractory Mass Provider, *Technical Data Sheet Of The Insulating Refractory Mass*. 2015.

[15] Refractory Mass Provider, *Technical Data Sheet Of The Silicon Carbide Refractory Mass*. 2015.

[16] M.Woite, "Properties of 16Mo3 steel." [Online]. Available: http://www.woite-edelstahl.com/15415en.html. [Accessed: 03-May-2016].

[17] Chemical Rubber Publishing Co., "Table of Emissivity of Various Surfaces."

[18] P. Saarenrinne, *Measurements in Thermal Scienses, MEI-71100, course material*. Tampere, 2015.

[19] Termorak, *Using and maintenance guide for refractory materials*. 2015.

[20] Thermocoupleinfo, "Type K Thermocouple Accuracy." [Online]. Available: http://www.thermocoupleinfo.com/. [Accessed: 23-Jun-2016].